Microbiology and Infectious Disease

The antigenic landscape of human influenza N2 neuraminidases from 2009 until 2017

Reviewed Preprint

Revised by authors after peer review.

About eLife's process

Reviewed preprint version 3
April 11, 2024 (this version)

Reviewed preprint version 2
March 4, 2024

Reviewed preprint version 1
October 9, 2023

Posted to preprint server
September 1, 2023

Sent for peer review
August 18, 2023

João Paulo Portela Catani, Anouk Smet, Tine Ysenbaert, Marnik Vuylsteke, Guy Bottu, Janick Mathys, Alexander Botzki, Guadalupe Cortes-Garcia, Tod Strugnell, Raul Gomila, John Hamberger, John Catalan, Irina V. Ustyugova, Timothy Farrell, Svetlana Stegalkina, Satyajit Ray, Lauren LaRue, Xavier Saelens, Thorsten U. Vogel

VIB Center for Medical Biotechnology, VIB, B-9052 Ghent, Belgium • Department of Biochemistry and Microbiology, Ghent University, B-9052 Ghent, Belgium • Gnomixx, Melle, Belgium • VIB Bioinformatics Core, VIB, B-9052 Ghent, Belgium • Sanofi, Research North America, Cambridge, Massachusetts, USA

https://en.wikipedia.org/wiki/Open_access

Copyright information

Abstract

Human H3N2 influenza viruses are subject to rapid antigenic evolution which translates into frequent updates of the composition of seasonal influenza vaccines. Despite these updates, the effectiveness of influenza vaccines against H3N2-associated disease is suboptimal. Seasonal influenza vaccines primarily induce hemagglutinin-specific antibody responses. However, antibodies directed against influenza neuraminidase (NA) also contribute to protection. Here, we analyzed the antigenic diversity of a panel of N2 NAs derived from human H3N2 viruses that circulated between 2009 and 2017. The antigenic breadth of these NAs was determined based on the NA inhibition (NAI) of a broad panel of ferret and mouse immune sera that were raised by infection and recombinant N2 NA immunization. This assessment allowed us to distinguish at least 4 antigenic groups in the N2 NAs derived from human H3N2 viruses that circulated between 2009 and 2017. Computational analysis further revealed that the amino acid residues in N2 NA that have a major impact on susceptibility to NAI by immune sera are in proximity of the catalytic site. Finally, a machine learning method was developed that allowed to accurately predict the impact of mutations that are present in our N2 NA panel on NAI. These findings have important implications for the renewed interest to develop improved influenza vaccines based on the inclusion of a protective NA antigen formulation.

eLife assessment

This study presents **valuable** data on the antigenic properties of neuraminidase proteins of human A/H3N2 influenza viruses sampled between 2009 and 2017. The antigenic properties are found to be generally concordant with genetic groups. Compared to a previous version, additional analyses have strengthened the work, with **solid** evidence supporting the claims of the authors.

Introduction

Neuraminidase (NA) and hemagglutinin (HA) constitute the two major antigenic proteins at the surface of influenza A and B virions (Uyeki et al., 2022). While HA mediates binding to sialic acids and membrane fusion, NA catalyses the removal of sialic acid residues from sialylated glycoproteins and glycolipids. This complementary role of HA and NA enables influenza virions to penetrate the mucus barrier that lines the respiratory epithelium and newly formed virions to be released from the infected cell (de Vries et al., 2020; Matrosovich et al., 2004; Palese et al., 1974). Immunity against influenza is associated with the presence of anti-HA antibodies in serum, as determined by a hemagglutination inhibition assay. In line with this, the composition of licensed influenza vaccines is primarily focused on the antigenic characteristics of HA as the protective vaccine antigen (Cox, 2013). Multiple studies, however, have underscored the protective potential of anti-NA immune responses as determined by NA inhibition (NAI) assays (Couch et al., 2013; Maier et al., 2019; Memoli et al., 2016; Monto and Kendal, 1973; Monto et al., 2015; Ng et al., 2019; Weiss et al., 2019). There is also evidence that pre-existing anti-N2 immunity induced by prior exposure to H2N2 viruses that circulated in the population from 1957 to 1968, tempered the impact of the H3N2 pandemic virus that emerged in 1968 (Eickhoff and Meiklejohn, 1969; Jester et al., 2020; Monto and Kendal, 1973; Viboud et al., 2005). Further, the pharmacological inhibition of NA activity is a well-established therapeutic strategy to try to reduce influenza severity and duration (Leneva et al., 2000; Yen et al., 2005). In addition, antibodies with NAI activity can protect against influenza virus infection in pre-clinical models (Chen et al., 2018; Deroo et al., 1996; Rosu et al., 2022; Wan et al., 2018; Wohlbold et al., 2017).

Since its appearance in 1968, human H3N2 viruses have been evolving faster than the co-circulating H1N1 and influenza B viruses (Bedford et al., 2014; Potter et al., 2019). The overall Influenza virus vaccine effectiveness varies between seasons and, despite frequent updates of the H3N2 HA component, the effectiveness of influenza vaccines against H3N2-associated disease ranges between 5 and 39%, which is lower than the effectiveness against H1N1 and influenza B (Belongia et al., 2016). In this context the use of NA as a complementary vaccine antigen might improve influenza vaccine effectiveness, for example by compensating for HA-based antigenic mismatches in circulating influenza virus strains (Krammer et al., 2018).

Phylogenetic analyses of HA and NA genes of human H3N2 viruses revealed the asynchronous evolution of the 2 proteins. In addition, the evolutionary rate as determined by the accumulation of mutations over time, is estimated to be 1.5 times lower for NA than for HA (Westgeest et al., 2012). Despite the strong evidence that immune responses directed against NA can contribute to protection against influenza, a comprehensive insight in the antigenic breadth and evolution of the H3N2 NA antigen is lacking (Nachbagauer et al., 2017; Rajendran et al., 2017; Smith et al., 2004; Westgeest et al., 2012).

Here, we determined the antigenic landscape of N2 NAs derived from human H3N2 strains that were isolated between 2009 and 2017. This analysis allowed the identification of at least 4 N2 NA antigenic groups and to estimate the weight of amino acid changes on their contribution to NA antigenic drift.

Results

Generation of H3N2-derived NA immune sera in ferrets and mice

Our aim was to determine the antigenic relationship between NAs derived from human H3N2 viruses that circulated during nearly one decade. We first selected 43 H3N2 neuraminidase protein sequences obtained via GISAID, derived from viruses that were isolated between 2009 and 2017 (Elbe and Buckland-Merrett, 2017). Hierarchical clustering with minimax linkage was employed to ensure the set was representative of overall protein sequence diversity (Bien and Tibshirani, 2011). Next, 43 recombinant H1N2 viruses were generated that carried the internal and HA genes from PR8 virus and the NA genes of the selected H3N2 viruses. In addition, the corresponding tetrabrachion-stabilized recombinant N2 NA proteins were produced in Chinese hamster ovary (CHO) cells and purified, and are referred to as NACHOs (Catani et al., 2022). All purified NACHOs were tetrameric based on SEC-MALS analysis. The enzymatic activity of the NACHOs was determined based on the hydrolysis of the fluorogenic small molecule substrate 4-methylumbelliferyl-N-acetylneuraminic acid (MUNANA). The NACHOs were active with a specific activity ranging from 0.27 to 27.48 nmole/min/µg, indicating correct folding and assembly of the NA head domains (**Table S1**).

Immune sera against all 43 H3N2-derived NAs were generated in pairs of ferrets by a primary infection with the respective H1N2 reassortant viruses. This prime by infection was used to avoid the use of an adjuvant upon subsequent boost with the corresponding NACHOs. On day 28 after primary infection, all animals were boosted by intramuscular injection of homologous NACHO, except for the ferrets that had been primed by infection with A/Stockholm/15/2014 and A/Estonia/91621/2015, which were re-inoculated with the same respective H1N2 reassortant viruses. These two pairs of ferrets were not boosted with homologous NACHO because the corresponding NACHOs were not available at the time of the experiment. Blood samples were taken from the ferrets on days 14 and 42 after (primary) infection (**Figure 1a**). Priming by H1N2 infection resulted in seroconversion against the respective immobilized homologous NACHOs (**Figure 1b**). Subsequent immunization with recombinant NACHOs boosted the NACHO-specific IgG titers in day 42 serum samples. In contrast, serum samples from the ferrets that had been re-inoculated with H1N2 reassortant carrying NA derived from A/Stockholm/15/2014 or A/Estonia/91621/2015, showed no further increase in titers, presumably because prior exposure with the same H1N2 virus had induced a sterilizing immune response (**Figure 1b**).

We also generated NA immune sera in BALB/c mice. Groups of 5 mice were immunized two times, with a two-week interval, by intramuscular injection with 1 µg of the respective 43 NACHOs adjuvanted with AF03. Blood was collected from the immunized mice and serum prepared on day 28 after the prime immunization (**Figure 1c**). NACHO-specific IgG titers in the mouse immune sera, pooled from each group, ranged from 1:8100 to 1:72900 (**Figure 1d**).

The antigenic profile of N2 neuraminidase

Next, NAI titers were determined in the ferret sera using a panel of H6N2 reassortant viruses in an enzyme-linked lectin assay (ELLA), avoiding interference by anti-H1 HA antibodies. We generated 27 H6N2 influenza viruses with H6 HA derived from A/mallard/Sweden/2002 and NA derived from a subset of the 43 H3N2 viruses, thereby retaining NA sequence diversity and year of H3N2 virus isolation (**Table S2**).

The 43 NAs used as antigens and 27 NAs as source of NA, could be classified into 4 groups when ordered according to the phylogenetic relatedness of their NA sequence (**Figure 2**). The conversion rate of MUNANA into 4-methylumbelliferyl and acetylneuraminic acid by these H6N2 viruses revealed a K_M that ranged from 20.7 to 144.8 µM as determined by the Michaelis-Menten

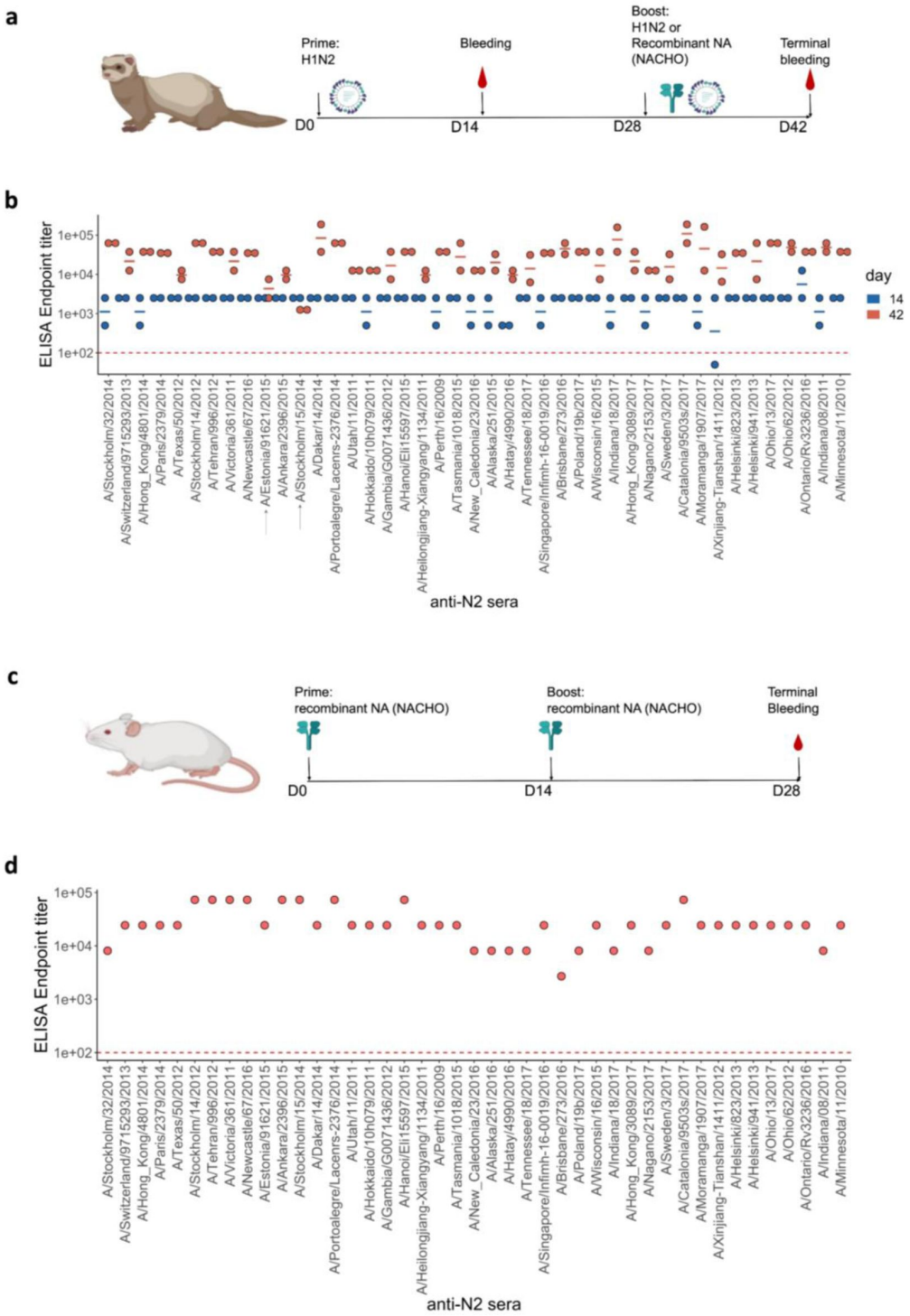

Figure 1.

Generation of anti-N2 sera panel from ferrets and mice.

(a) 43 Ferret immunization and blood sampling scheme. The second immunization on day 28 was performed with homologous NACHO except for the ferrets that had been primed with $H1N2_{A/Estonia/91621/2015}$ or $H1N2_{A/Stockholm/15/2014}$, which were infected again on day 28 post prime with the same H1N2 viruses. (b) Homologous NACHO ELISA titer of ferret sera sampled on day 14 after inoculation with H1N2 virus and 2 weeks after the boost with recombinant NA or by re-inoculation with $H1N2_{A/Estonia/91621/2015}$ or $H1N2_{A/Stockholm/15/2014}$ (indicated by arrows on the X-axis). (c) 43 BALB/c mouse immunization and blood sampling scheme. (d) Homologous NACHO serum IgG titers in pooled sera from mice that were immunized twice with recombinant NA. Mouse and ferrets representations were created with *BioRender.com* (2023).

equation (**Figure 2 – figure supplement 1a** and **Table S2**). Interestingly, the K_M differs between the distinct phylogenetic groups (**Figure 2 – figure supplement 1a**). There was a negative correlation between the K_M values and the dilution of the H6N2 viruses required to set the 70% maximal NA activity in ELLA (**Figure 2 – figure supplement 1b**).

Using this panel of 27 H6N2s, we determined the NAI titers in the sera obtained from the 43 pairs of ferrets 2 weeks after the boost. ELLAs were performed in duplicate for all serum samples against one H6N2 target at the same time. The reciprocal NAI titers of the ferret sera paired with H6N2 viruses are shown in **Table S3**. In general, the NAI titers of the ferret sera were the highest against homologous and phylogenetically closely related H6N2 viruses. In **Figure 2**, all the tested ferret sera are represented in the rows and the 27 H6N2 viruses against which the sera were evaluated in ELLA are presented in the columns. The serum samples were ordered according to the phylogenetic relatedness of the N2 NA head domain amino acid sequences, showing that these cluster in 4 groups (G1-G4). The ELLA-based IC_{50} NAI titers were normalized by the homologous ELISA titers and then plotted relative to the maximum NAI titer obtained against the respective H6N2 target viruses. The heatmap thus represents, for each H6N2 virus, the normalized ELLA IC_{50} titer expressed as $\log_2$ of the fold-difference relative to the serum with the highest IC_{50} value against that H6N2 virus (dark red squares indicate high and blue squares low IC_{50} values) (**Figure 2**).

Next, these normalized NAI values were clustered against each of the H6N2s using the Unweighted Pair Group Method with Arithmetic Mean (UPGMA), which is a distance-based method. This clustering allowed to discern at least 4 major antigenic clusters (AC1 to −4) that are depicted at the top of the heat map (**Figure 2**). It is interesting to note that the H6N2 viruses with NA antigens derived from A/Wisconsin/16/15 and A/Alaska/251/15 do not segregate into AC2, as would be predicted based on the phylogenetic relatedness, but cluster in AC1 based on the UPGMA. However, the overall concordance of the antigenicity with the phylogenetic relatedness, based on the amino acid sequences of the NA head domains, was confirmed by hierarchical clustering with bootstrapping and k-means (**Figure 2 – figure supplements 2a** and 2b).

In addition, antigenic cartography analysis, based on the method described by Smith *et al.* (Smith et al., 2004), resulted in a antigenic map of the N2 NAs that was in line with the 4 proposed antigenic clusters (**Figure 2 – figure supplement 3**).

In line with this, a positive correlation was observed between the pairwise phylogenetic distances and the normalized NAI IC_{50} values for each of the tested H6N2s (**Figure 2 – figure supplement 4**).

We further tested the NAI activity of ferrets' sera obtained 2 weeks after the prime infection against at least one H6N2 virus from each antigenic cluster. These H6N2 viruses were selected based on their antigenic relatedness as deduced from the ferret immune sera analysis (**Figure 2**) with 2 representatives from group 1 (Tex12, and Per09) and 1 each from group 2 (Kan17), group 3 (Hel823), and group 4 (Ind11). The normalized data confirmed the antigenic clustering observed in sera after boost (**Figure 2 – figure supplement 5**).

The NAI titers were also determined in the sera obtained from the 43 groups of NACHO-immunized mice against 7 of the H6N2 viruses (**Figure 2 – figure supplement 6a**). These H6N2 viruses were selected as described above with the addition of HK14 and Swi13 H6N2s, both belonging to antigenic cluster 1. Serum NAI IC_{50} values against a given H6N2 virus were normalized against the IC_{50} of the mouse serum that had the highest NAI titers against the tested H6N2 virus. UPGMA-based clustering showed that the mouse NACHO immune sera displayed a similar recognition pattern as the ferret immune sera that had been generated by H1N2 priming

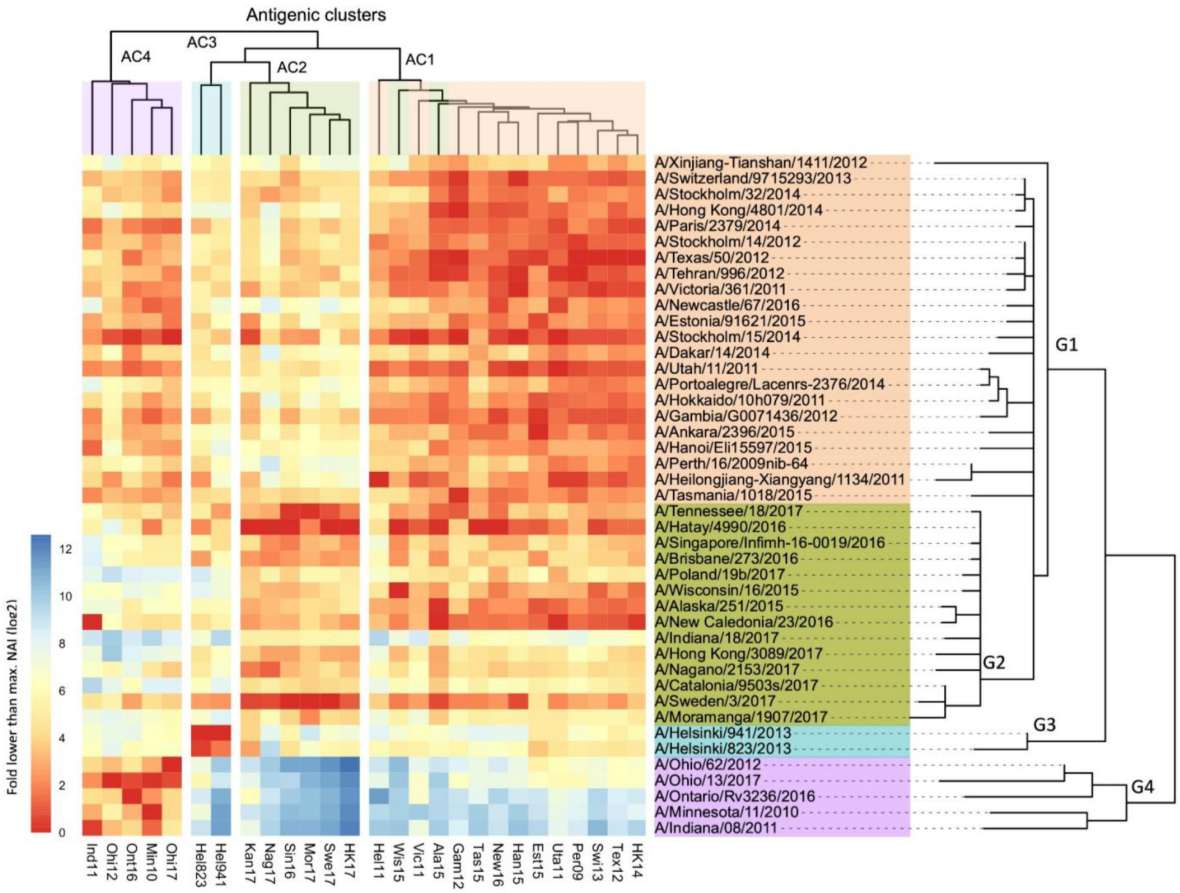

Figure 2.

Breadth of N2 NA inhibition.

43 Phylogenetic tree based on the N2 NA head domain amino acid sequences and heat-map representing the average of normalized neuraminidase inhibition per H6N2 [$\log_2$ (max (NAI/ ELISA homologous titer)/(NAI/ homologous ELISA titer)] determined in ferret sera after the boost (listed vertically). The red-to-blue scale indicates high-to-low NAI observed in ELLA against the H6N2 reassortants (listed at the bottom). UPGMA clustering of H6N2s inhibition profiles are shown on top of the heat map and coloured according to the phylogenetic groups.

followed by a NACHO boost (**Figure 2**). For example, HK14 H6N2 NA activity is strongly inhibited by sera from group 1, is poorly inhibited by most of the sera from group 2 and is hardly inhibited by group 3 and 4 sera from both ferrets and mice.

Ind11 H6N2 NA activity, on the other hand, was inhibited by group 1 and 4, and hardly by group 2 and 3 immune sera. Overall, the normalized NAI IC_{50} values of the ferret and mouse immune sera correlated very well with coefficients values ranging from 0.33 to 0.78 (**Figure 2 – figure supplement 6b**).

Association analysis reveals amino acid residue substitutions that strongly impact NAI

NA of human influenza viruses is subject to antigenic drift, predominantly driven by the NAI activity that is detectable in the host serum (Air et al., 1985; Yasuhara et al., 2019). There are a total of 102 amino acid differences between the head domains of the NAs that were used to generate the 43 ferret immune sera (**Figure 3 - Figure supplement 1**). These 102 variable amino acids in the N2 head domain are predominantly exposed on the NA surface (**Figure 3 – figure supplement 2**).

To try to identify which of these amino acid substitutions have a significant impact on NAI, we performed an association analysis for each of the tested H6N2 viruses. For this analysis, the NAI IC_{50} value was compared between groups of N2 sera according to the presence or absence of a substitution of any of the 102 amino acid position that are different between the panel of 43 tested N2s against which sera had been raised in ferrets. As a result, a p-value is obtained for each position that reflects its possible impact on NAI (**Figure 3a**). The significance values higher than 1.3 ($p<0.05$) of representative strains of the 4 antigenic groups were represented on the surface of N2 (**Figure 3b**). No obvious antigenic patches, however, could be distinguished on the N2 NA surface.

A similar association analysis was performed using the NAI values obtained with the mouse NACHO immune sera. The calculated p-values obtained from the mouse and ferret NAI data were in line with each other (**Figure 3 – figure supplement 3**).

Residues close to the catalytic pocket are more likely to impact NAI

We next calculated the distance between the Cα atom of each amino acid present in the N2 structure (PDB: 6BR6, from A/Perth/16/2009 NA) to each Cα of the variable amino acids present in the panel. We then determined the correlation of those distances with the p-values that were previously determined in the association analysis. The resulting correlation coefficients (Tau values) indicate a similar pattern among all 27 tested H6N2s (**Figure 4a**). When visualized on the N2 surface structure, the Tau values revealed a geometrical distribution with the negative correlations being in closer proximity to the catalytic pocket (**Figure 4b**). Similar data was obtained when mice sera were analyzed this way (**Figure 4 – figure supplement 1**).

Prediction of the N2 antigenicity based on a machine learning method

The antigenic drift of human H3 HA has been extensively studied and modelled (Meyer and Wilke, 2015; Smith et al., 2004; Westgeest et al., 2012; Wu et al., 2020). To model the NA drift observed in our panel of N2 NAs, we first calculated the antigenic distances between the distinct NA sera, using a similar approach as has been used to visualize the HA antigenic map (Cai et al., 2012). Then, using the antigenic distances and a random forest method (RF), a model was built

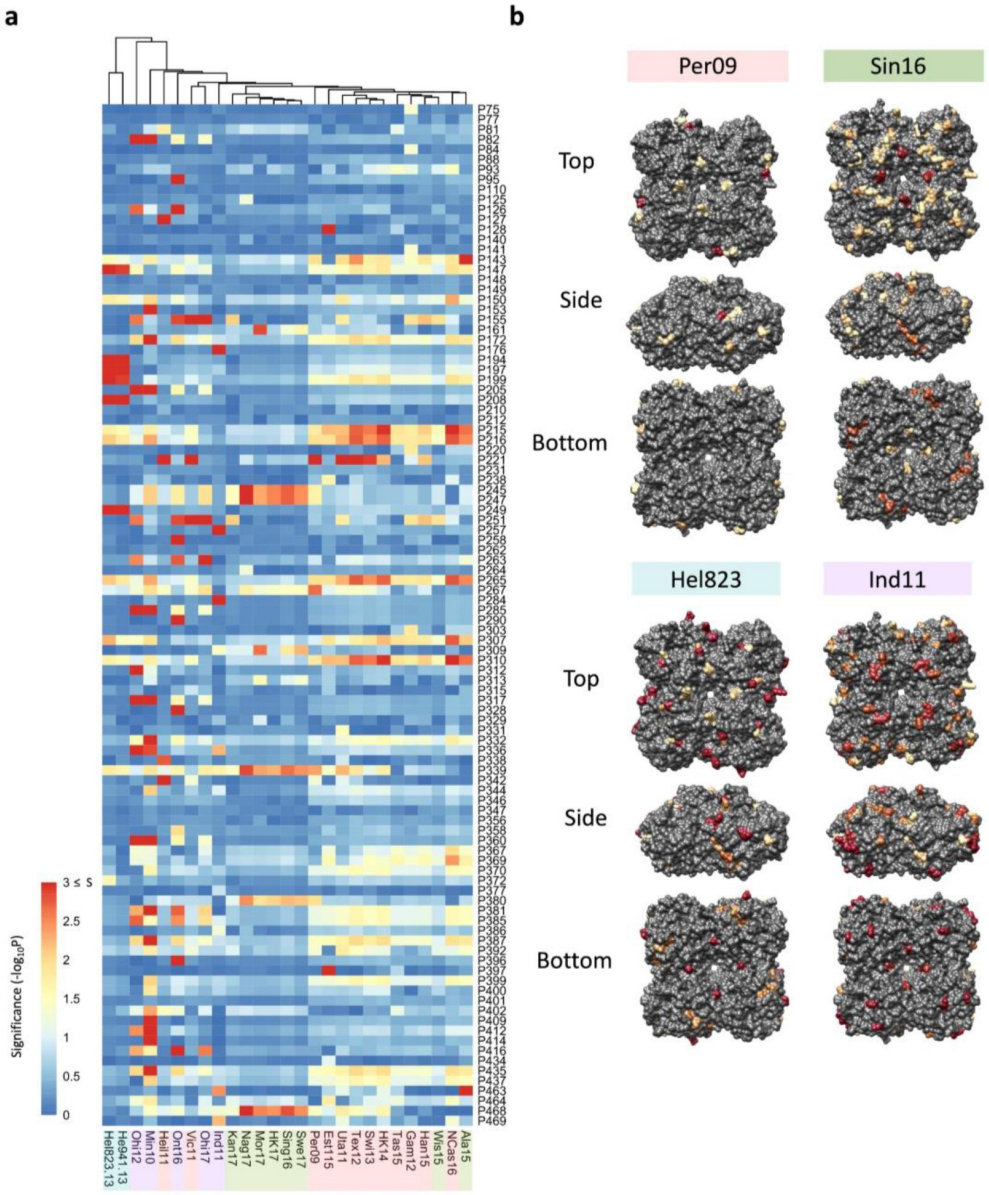

Figure 3.

Association analysis reveals impact of amino acid mutations on NAI.

(a) Association study performed for each H6N2 virus (listed at the bottom) to determine the probability of each variable amino acid (listed on the right) present in the panel of 43 NAs to impact the NAI. The red-to-blue scale represents significance values ($S=-\log_{10}P$) associated with each amino acid substitution. The dark red in the color scale represent all values that are equal or higher than 3 (corresponding to p-values ≤ 0.001). The colour shades on the bottom side indicate the distinct phylogenetic groups. (b) The significant values ($p<0.05$) were represented on the surface of N2 tetramer (PDB accession number 4H53) for one representative strain of each phylogenetic group with a yellow to red scale of significance ($-\log_{10}P$).

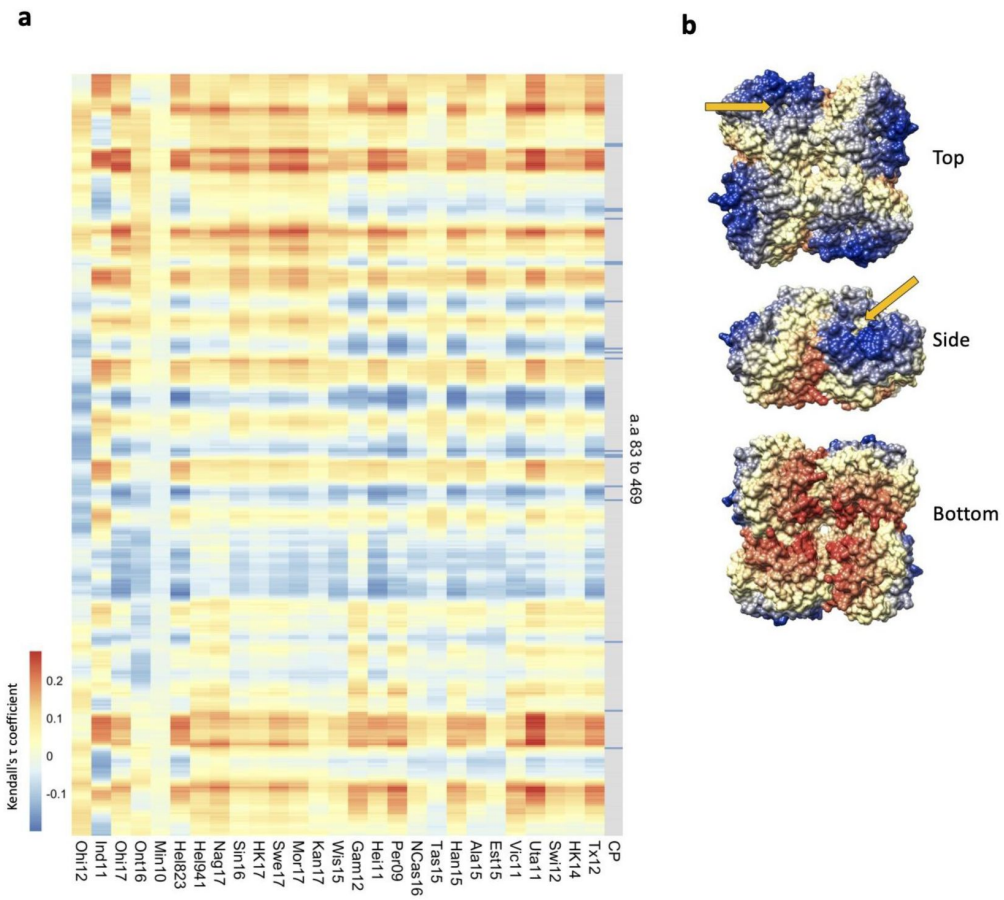

Figure 4.

Residues close to the catalytic pocket are more likely to impact NAI.

(a) Significance values (102 variable amino acids) obtained from the association study were correlated to the distance between every amino acid and each of the variable amino acids in the NA structure. The red-to-blue scale represents the Tau values obtained in the Kendall correlation. Amino acids 83 to 469 are shown from top to bottom in the heatmap. The H6N2s used in the NAI panel are listed at the bottom. The grey column indicates the residues that are part of the catalytic pocket (CP) that directly interact with the substrate (R118, D151, R152, R224, E276, R292, R371, and Y406) and the residues that play a key role in stabilizing the catalytic site (E119, R156, W178, S179, D198, I222, E227, H274, E277, N294, and E425). (b) Tau values obtained from Tex12 H6N2 correlation are represented on the surface of the N2 structure of A/RI/5+/1957 (PBD 4H53), the arrow indicates the catalytic pocket in one NA protomer.

based on amino acid sequence information. A similar model has been used by Yao *et al*. to predict the antigenicity of H3 HA (Yao et al., 2017). Here, the optimized model was built using a combination of 25 randomly sampled features in 1500 decision trees. The resulting model generates predictive antigenic distances that strongly correlate with the observed values (**Figure 5a**), with an RMSE/mean=0.207). The RF also enables scoring of amino acid residues according to their importance in the decision trees. One measure of importance can be defined as how early a change in a position is placed in the generated decision trees (mean minimal depth). Another measure of importance is how much the standard error mean increases when a variable is permuted. Finally, the prevalence of a variable amino acid in nodes of the decision tree can also indicate its importance. Those importance scores were represented in a multi-way plot (**Figure 5b**). The importance scores highlighted similar positions as previously determined in the association study. Finally, we used NA sequences of recent seasonal influenza vaccine recommended H3N2 strains to predict their antigenic distance relative to our panel of N2s, including 3 recent N2 NA components (from A/HongKong/45/2019, A/Tasmania/503/2020, and A/Darwin/6/2021) that were not present in our data set. The predicted antigenic distances were plotted in the heatmap in a red to blue scale, indicating high to low antigenic distance, respectively (**Figure 5c**). The RF clearly reproduced the drift observed in AC2 versus AC1. The modelling also indicates that the antigenic distance of the 3 recent N2s to their corresponding group 2 NAs is increasing (represented by the dark blue turning light blue, from the A/Singapore/infimh-16-0019/2016 towards the A/Darwin/6/2021 in G2) whereas their distance to group 4 NAs is decreasing (dark red becoming yellow from the A/Singapore/infimh-16-0019/2016 towards the A/Darwin/6/2021 in G4).

Discussion

The sequence diversity of N2 proteins derived from the 43 selected human H3N2 viruses isolated between 2009 and 2017 allows to classify them in 4 major phylogenetic groups. Group 1 contains 22 N2 NAs, 4 of which were derived from vaccine recommended H3N2 strains: A/Perth/16/2009, A/Texas/50/2012, A/Switzerland/9715293/2013, and A/Hong Kong/4801/2014. Phylogenetic group 2 comprises 14 N2 NAs, one of which is derived from a vaccine H3N2 recommended strain:

A/Singapore/INFIMH-16-0019/2016. The third phylogenetic group contains two NAs that are derived from H3N2 strains that had been isolated in Helsinki in 2013. Remarkably, the NA sequence of these two strains is closely related to that of H3N2s that circulated more than 15 years earlier (e.g. 99% identity with NA of A/Sydney/5/1997). The fourth phylogenetic group is composed of NAs derived from zoonotic cases with swine H3N2 strains isolated between 2012 and 2017. Swine-to-human transmission of H3N2 viruses have occurred multiple times in the USA in 2012 and continue to be detected at low frequency until to date (CDC, 2023; Elbe and Buckland-Merrett, 2017).

We assessed the antigenic diversity of the NA panel by generating 27 recombinant H6N2 viruses and 43 ferret NA immune sera produced by H1N2 priming followed by boosting with homologous recombinant NA (NACHO; n = 41) or by reinfection with H1N2 (A/Estonia/91621/2015 and A/Stockholm/15/2014). Most of the ferrets had detectable serum anti-N2 antibodies by day 14 after infection with H1N2. Anti-NA antibody titers increased after a boost with non-adjuvanted homologous recombinant CHO-produced soluble tetrameric NA suggesting that the use of recombinant NA may boost naturally acquired anti-NA antibody responses in the human population.

The NAI activity of the ferret sera against 27 tested H6N2s reassortants revealed a pattern of inhibition that largely coincides with the phylogenetic distances based on the NA head domain sequences. In the tested panel of H6N2s, at least 4 major antigenic groups were identified. We noted that H6N2 with Kan17 NA had a broader profile of inhibition than other H6N2 viruses from

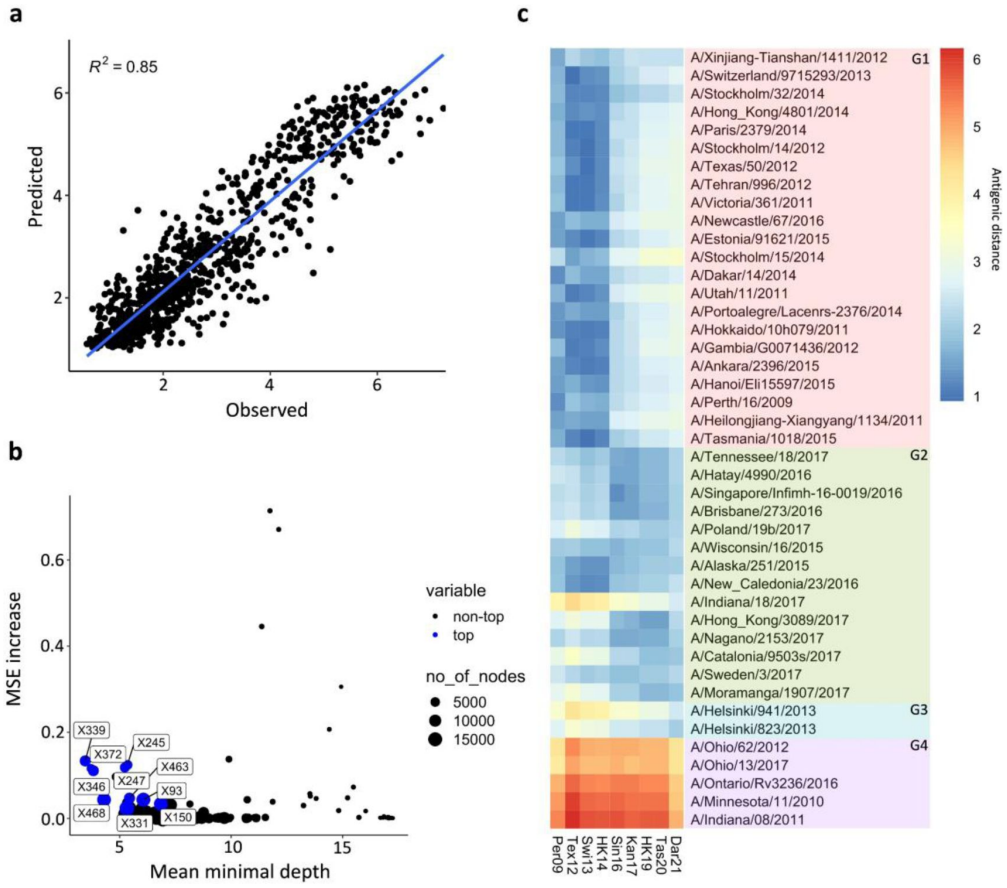

Figure 5.

Prediction of N2 antigenicity based on machine learning.

(a) Predicted *vs* observed normalized NAIs are shown. (b) Multi-way importance plot indicating the increase in mean standard error, the mean depth, and number of nodes. The top 10 most important amino acid changes are highlighted in blue and annotated with their position in the NA sequence. (c) 43 The heatmap indicates the predicted antigenic distances of N2s from recent H3N2 isolates (at the bottom of the heatmap) relative to the N2s that were used in the NAI breadth panel (listed vertically). The antigenic distances were calculated based on NA protein sequence.

group 2, being also inhibited by serum raised against NA from phylogenetic groups 3 and, to a lesser extent, group 4. Additionally, the H6N2s Wis15 and Ala15 have an antigenic behaviour that is more closely related to antigenic cluster 1, despite belonging to group 2 according to their phylogenetic similarities. Based on the NAI panel, an association analysis was performed to try to identify amino acid changes that affect NAI. It is interesting to note that the amino acid substitutions S245N and S247T, combined with substitution P468H, were identified in this association analysis. Those substitutions were described as major contributors of the NA antigenic drift that occurred in H3N2 in 2014 (Wan et al., 2019). NAs from A/Wisconsin/16/2015 and A/Alaska/251/2015 also have the S245N and S247T substitutions and phylogenetically belong to group 2 NAs. However, those 2 NAs lack the P468H mutation and are antigenically closer to group 1 NAs, confirming the requirement of P468H combined with the S245N and S247T substitutions for this NA antigenic drift (Wan et al., 2019). This observation suggests that NA antigenic drift may sometimes require a combination of amino acid changes rather than single mutations. Wang and colleagues have very elegantly demonstrated that N2 antigenic evolution is constrained by charge balances in an antigenic region, which can partially explain the observation that NA amino acids can undergo co-evolution to result in antigenic drift (Wang et al., 2021). Interestingly, NAs originated from H3N2 variants classified in phylogenetic group 4 were antigenically closer to N2s belonging to phylogenetic group 1. This suggest that the antigenic drift of recent NAs from group 2 increases the antigenic distance from the N2s of swine origin.

Noteworthy, the analysis of the sera obtained from ferrets after infection shows that, despite the lower homologous anti-NA titers, the inhibition pattern evaluated against 5 distinct H6N2s (composed of at least one representative of each antigenic group) is in accordance with the response obtained after boosting with recombinant protein. This suggests that a boost with homologous recombinant soluble tetrameric NA does not alter the breadth of the antibody response induced by H1N2 infection only. Nevertheless, we cannot exclude a degree of increased cross-reactivity of the sera from NACHO278 boosted ferret. It has been reported that repeated H3N2 virus exposure of ferrets affects anti279 hemagglutinin responses (Kosikova et al., 2018)

NAI was also determined against 7 distinct H6N2 reassortant viruses using a panel of 43 anti-N2 NA sera raised in mice by immunization with adjuvanted NACHOs. The observed NAI responses again allowed clustering of the N2 NAs into 4 main antigenic groups, which correlates with data obtained in ferrets. Studies in mice can thus offer a convenient alternative to the use of ferrets in future NA antigenicity studies. This data also supports the hypothesis that there may be universal rules of immunogen antigenicity and immunogenicity (Altman et al., 2015).

The determined K_M values of the H6N2 viruses used here, indicates that substrate affinity tends to vary according to the phylogenetic relatedness of N2s. The N-glycosylation at position 245 was previously described to be responsible for reducing N2 affinity for its substrate (Powell and Pekosz, 2020). Unlike group 2, which is primarily characterized by the presence of a N-glycan at position 245, NAs from phylogenetic group 4 have a low K_M, indicating an increased affinity for substrate. This result suggests that phylogenetic drift can be accompanied by changes in NA enzymatic properties. Curiously, the Ala15, Wis15, and Kan17, despite having antigenic properties closer to group 1, still have K_M values that are comparable to those of group 2 N2 NAs.

After the determination of NA antigenic distances, we used random forest modelling to estimate the impact of amino acid changes on antigenic distances. We obtained a strong correlation of predicted versus observed antigenic distances. However, it is important to note that the training dataset was based on the 102 mutations present in our panel, limiting the predictions for other positions. Furthermore, random forest enabled the classification of the variable amino acids according to importance scores. Also, our modelling does not consider that substitution by other amino acids can have a distinct impact on the antigenic distance. As a consequence, predictions based on the model could underestimate the importance of a particular amino acid residue substitution in some cases. It is important to highlight that co-occurring substitutions in our panel

(the ones present in the main branches of the phylogenetic tree) cannot be individually assessed by association analysis or the random forest model. The individual weight of those mutation on NA drift thus remains to be experimentally demonstrated. Interestingly, the modelling could put in evidence the gradual drift of recent N2s which were not present in the dataset (A/Hong Kong/45/2019, A/Tasmania/503/2020, and A/Darwin/6/2021).

It has been reported that an N-glycosylation site at position 329 combined with E344 in NA from human H3N2 viruses from 2007 to 2013 was gradually lost in later H3N2 viruses (Ge et al., 2022). This loss of an N-glycosylation site at position 329 combined with an E344K substitution was associated with a change in NAI reactivity in ferret sera. Three N2 NAs in our panel, derived from A/Victoria/361/2011, A/Hong_Kong/3089/2017, and A/Tennessee/18/2017, lack this N-glycosylation motif. The E344K substitution is present in three other NAs, derived from A/Nagano/2153/2017, A/Minnesota/11/2010, and A/Indiana/08/2011. The importance of those mutations is among the lowest ones predicted by our modeling. However, the differences in NAI reported by Ge *et al.* are very modest (less than twofold). The experimental variability in our study potentially limits the identification of substitutions with a subtle impact on NAI.

The protective potential of NA antigen against influenza has been underscored by multiple studies. It is likely that NA will be included as a standard component of next generation influenza vaccines. The difficulties of producing stable tetrameric NA may be overcome in the future thanks to protein design or with the advent of mRNA-based vaccines (Catani et al., 2022; Chivukula et al., 2021; Ellis et al., 2022). The antigenic modelling associated with sequence surveillance may increase our predictive ability, highlighting major potential drifts and support NA antigen designs that may elicit broader NAI responses compared to natural NA.

In summary, our study shows that immunization with recombinant N2 NA immunogen can boost anti-NA serum antibody responses in ferrets that were primed by infection with an influenza virus that carries the homologous NA. At least 4 major antigenic groups could be distinguished in N2 NA derived from human H3N2 viruses that were isolated between 2009 to 2017, and those antigenic groups predominantly correspond with the phylogenetic relatedness of the N2 head domains. In addition, the amino acid substitutions in close proximity of the NA catalytic pocket are more likely to affect NAI patterns.

Material and Methods

Rescue of H1N2 and H6N2 reassortants

All reassortant H1N2 and H6N2 viruses included in the study were generated by reverse genetics, with each reassortant expressing the targeted NA antigen, internal genes from A/Puerto Rico/8/1934 H1N1 (PR8), and the HA from PR8 H1N1 or A/mallard/Sweden/81/2002 H6N1, respectively. Briefly, HA and NA segments including non-coding regions were generated by custom gene synthesis (Geneart AG), while PR8 internal segments were derived from a viral isolate as previously published (Marsh and Tannock, 2005). All segments were cloned into a bi-directional transcription plasmid derived from pUC57 (Genscript) including polymerase (Pol) I and Pol II promoters, as previously described (Hoffmann et al., 2000), and the entire set of 8 plasmids was used to transfect 293FT cells (Thermo Fisher Scientific) using Lipofectamine 2000 CD (Thermo Fisher Scientific). Twenty-four hours after transfection, Madin-Darby Canine Kidney Cells (MDCK-) ATL cells (ATCC) were added to the transfected cells in the presence of TPCK-treated trypsin (Sigma) to allow influenza virus propagation. Cell culture supernatants containing influenza virus were harvested 7 days post-MDCK addition and blindly passaged in 8–10-day-old embryonated chicken eggs (Charles River Laboratories, Inc.). Inoculated eggs were incubated at 37°C for 48 h, then cooled to 4°C for 12 h, prior to allantoic fluid harvest and clarification by low-speed

centrifugation (3,000 rpm, 20 min). For H6N2 viruses only, high-yield stocks were generated by an additional passage in eggs as described above. Virus titers were determined by plaque assay on MDCK cells.

Design and production of recombinant proteins

The coding information of the NACHO proteins was cloned under the transcriptional control of the CMV promoter in the pCDNA3.4 plasmid with a CD5 secretion signal, an amino-terminal His-tag and the thrombin cleavage signal followed by tetrabrachion-NA. NACHOs were expressed in a mammalian cell culture system as previously described with modifications (Catani et al., 2022).

Animal experiments

The ferret immunization experiment was conducted at Bioqual, Inc., MD (USA). The experiments were approved by the Institutional Animal Care and Use Committee of the Bioqual (reference number 17-021.6). Outbred 18-22 weeks old naïve male and female Fitch ferrets were obtained from Triple F, PA (USA) and housed under specified pathogen-free conditions with food and water *ad libitum*. Ferrets were primed on day 0 by intranasal challenge with influenza H1N2 reassortant virus (1,000µl/dose, split evenly between nostrils). Four weeks after initial infection (day 28), ferrets were immunized with 45 µg of NACHO (500µl/dose, intramuscularly, split evenly between hind thighs) corresponding to homologous NA used in day 0 prime. Alternatively, and due to low yield of selected recombinant NACHOs, ferrets were boosted on day 28 with 15 µg of homologous NACHO (A/Perth/16/2009nib-64, A/Tasmania/1018/2015, A/Utah/11/2011, and A/West Virginia/17/2012) or were inoculated with the same H1N2 reassortant virus used in the prime (A/Estonia/91621/2015 and A/Stockholm/15/2014). Sera from bleeds two weeks after the prime (day 14) and booster vaccination (day 42) were tested for immunogenicity and seroconversion in serological assays.

The mouse immunization experiments were conducted according to the Belgian legislation (Belgian Law 14/08/1986 and Belgium Royal Decree 06/04/2010) and European legislation on protection of animals used for scientific purposes (EU directives 2010/63/EU and 86/609/EEC). Experimental protocols were all approved by the Ethics Committee of the Vlaams Instituut voor Biotechnologie (VIB), Ghent University, Faculty of Science (EC2019-035). Female BALB/c mice, aged 6–7 weeks, were purchased from Charles River. The mice were housed in a specified pathogen-free animal house with food and water *ad libitum*. Animals were immunized intramuscularly in the right quadriceps. Immunization was performed with 50 µl containing 1 µg of recombinant protein (tetrabrachion stabilized NAs, referred to as NACHOs). All, except A/West Virginia/17/2012 NACHOs were used as immunogens in mice. All immunizations were adjuvanted with a 1:1 volume of AF03 (25 µl of antigen in PBS + 25 µl of AF03 per dose) (Caillet et al., 2010).

Two or three weeks after the boost immunization, mice were humanely sacrificed with an anaesthetic overdose of Nembutal (6 mg per mouse) and bled retro-orbitally. The obtained blood samples were incubated for 30 min at 37°C to allow clotting, which was followed by centrifugation at 10,500 g for 5 minutes. The supernatant (the serum) was recovered and submitted to a second centrifugation at 10,500 g for 5 minutes. Cleared sera were stored at −20°C before use in serological assays.

Elisa

Anti-tetNA IgG levels in mouse and ferret sera were determined by capture ELISA using tetNAs in Pierce™ nickel-coated plates (cat. # 15442). Recombinant proteins were diluted in DPBS (Life technologies cat. # 14040-182) (tetNA was diluted to 0.5 µg/ml). Then, 50 µl of the coating antigen solutions was added to each well and the plate was incubated at room temperature for 1 h on a shaking platform. The wells of the plates were then washed 3 times with PBS-T (Sigma cat. # P3563-10PAK) and blocked for 1h with 1% BSA (for the mouse sera) or 10% milk (for the ferret sera) in

DPBS. After blocking, the wells of the plates were washed once with PBS-T and incubated with a 3-fold serial dilution, starting at a 1/100 dilution, of serum in DPBS, 0.5% BSA, 0.05% tween-20 for 2h at room temperature on a shaking platform. The wells of the plates were then washed 5 times with PBS-T and incubated with a 1:5000 dilution of anti-mouse IgG-HRP (GE healthcare cat. # NA931-1ml), or with a 1:100000 dilution of anti-ferret IgG-HRP (Abcam cat. # 112770) in DPBS, 0.5% BSA, 0.05% Tween-20. The 3,3',5,5'-tetramethylbenzidine (TMB) substrate (BD cat. # 555214) was added after 3 washes with PBS-T and the reaction was stopped after 5 min by addition of 50 µl of 1 M H_2SO_4. The optical density (O.D.) in each well was determined at 450 nm and, as a reference, 655 nm using an iMark™ Microplate Absorbance Reader (Bio-rad). The end point titer was determined for each serum sample by scoring the dilution that resulted in an O.D. that was equal to or 2 times higher than the background O.D. obtained from pre-immune control sera dilution series.

Enzyme-linked lectin assay to determine neuraminidase inhibition titers

Fetuin (Sigma cat. # F3385) was diluted into coating buffer (KPL cat. # 50-84-01) to a concentration of 25 µg/ml and 50 µl was added to the wells of Nunc MaxiSorp™ plates (Thermofisher cat. # 44-2404-21), which were incubated overnight at 4°C. The coated plates were then washed 3 times with PBS-T (Sigma cat. # P3563-10PAK) and incubated overnight with 60 µl of a dilution of H6N2 and 60 µl of 2-fold serial dilution of serum, starting at a 1/20 dilution, in sample buffer (1X MES VWR cat. # AAJ61979-AP: 20mM $CaCl_2$, 1% BSA, 0.5% Tween-20). These dilutions of the H6Nx viruses correspond to the 70% maximum activity of NA from the respective viruses as determined in the ELLA assay. Fetuin-coated plates were then washed 3 times with PBS-T and incubated for 1 h with a solution of PNA-HRP (cat. # L6135-1MG, Sigma) at 5 µg/ml in conjugate diluent (MES pH 6.5, 20 mM CaCl2, 1% BSA). The plates were washed 3 times with PBS-T, TMB substrate was added and then the plates were incubated for 5 minutes before the reaction was stopped by the addition of 50 µl of 1 M H_2SO_4. The optical density was measured at 450 nm and, as a reference, 655 nm in an iMark™ Microplate Absorbance Reader (Bio-rad). Half maximum inhibitory concentrations (IC_{50}) values were determined by non-linear regression analysis (GraphPad Prism software).

NA Enzyme Kinetics Assay

The enzymatic activity of NACHOs and H6N2s was determined with the fluorogenic small substrate 4-methylumbelliferyl)-α-d-*N*-acetylneuraminic acid (MUNANA) as previously described (Marathe et al., 2013). First H6N2 dilutions were tested to ensure that MUNANA conversion into 4-methylumbelliferone (4-MU) generated fluorescence over time at a linear ratio. Ten microliters of 1 mM of MUNANA (Sigma cat # M8639) in 200 mM sodium acetate buffer (pH 6.5) containing 2 mM $CaCl_2$ and 1% butanol was incubated with 40 µl of PBS solution containing viral dilution. Conversion to 4-MU was monitored every 2 min for 1 h using a BMG Fluostar OPTIMA reader (excitation at 365 nm and emission determined at 450 nm). Second, using the selected dilution of virus, the assay was repeated with dilutions of MUNANA ranging from 2.5 to 100 µM. A standard curve with 800 to 25 pmoles/well of 4-MU (Sigma cat # M1508) was used to extrapolate the molar conversion of MUNANA. K_M was calculated using GraphPad Prism version 8.4.3.

Antigenic cartography

Antigenic cartography was performed as described by Smith et al. (Smith et al., 2004) using the R CRAN package (*https://CRAN.R-project.org/package=Racmacs*). The antigenic map was optimized 5000 times and the best optimization was kept (stress value=1366,47). Uncertainty was measured by bootstrapping 1000 repeats with 100 optimizations per repeat.

Association study

For the association analysis, under the assumption of homogeneous genetic relatedness among the selected H3N2 virus strains, a simple linear regression model for mutation-trait association analysis was fitted to the data for each H6N2 separately. The significance values were calculated by comparing IC_{50} values of sera that were classified into 2 groups according to the presence or absence of variation in the amino acid of reference Tex12 sequence.

Correlations with distances from the NA catalytic pocket

Tau values were determined by correlating distances with significance values obtained from the association analysis or the importance scores obtained from machine learning. A similar method was described by Meyer *et al.* to define geometrical constraints of HA evolution (Meyer and Wilke, 2015). Briefly, the relative distances of amino acids were calculated based on the structure of A/Perth/2009 (H3N2) NA (PDB: 6BR6) (Hadházi et al., 2018). The distances were calculated from each Cα to every other Cα. The distances from every residue to the 98 variable residues (4 of the 102 variable amino acids are localized near the end of the stalk and are not resolved in the crystal structure) residues of the that are present in the panel of N2s and the 6BR6 structure were then correlated with the significance values that were obtained in the association analysis, or importance scores obtained in the machine learning. Correlation coefficients were visualized on the structure of N2 NA derived from pandemic A/RI/5+/1957 H2N2 virus (PDB: 4H53)(Vavricka et al., 2013) using Chimera 1.14.

Random Forest algorithm

The Random Forest algorithm was adapted from (Yao et al., 2017). Briefly, the non-conserved positions in the multiple sequence alignment of N2 head domain amino acid sequences of all tested N2s were selected. The feature matrix (X) was created by assessing matches/mismatches on each non-conserved position for each pair of N2 head domain amino acid sequences as:

$$X = \begin{array}{c} \\ V_1V_2 \\ \vdots \\ V_1V_n \\ \vdots \\ V_{n-1}V_n \end{array} \begin{array}{c} \begin{array}{cccc} X_1 & X_2 & \cdots & X_m \end{array} \\ \begin{array}{cccc} 0 & 1 & \ldots & 1 \\ \vdots & \vdots & \ldots & \vdots \\ 1 & 0 & \ldots & 1 \\ \vdots & \vdots & \ldots & \vdots \\ 1 & 0 & \ldots & 1 \end{array} \end{array}$$

where X_i represents the non-conserved positions in the multiple sequence alignment

m is the number of non-conserved positions (102 in total)

V_i represents the N2 head domain sequence for each tested NA

n is the number of tested sera (43 in total)

0 represents a match, 1 represents a mismatch in the alignment

The response vector (Y) is composed of the antigenic distances for each pair of tested sera. These antigenic distances were determined based on NAI, similarly to the method used to determine HI based immunogenic distances that was described by Cai *et al.* In summary, the distances between sera was calculated as $\frac{1}{n}\sum_{t=1}^{n}|d[t,i]-d[i,t]|$, which represent average distances between 2 serum samples among all tested H6N2s (Cai et al., 2012). We applied the random forest function from the randomForest package in R to construct the model. We set the bootstrapping (tree) number to 1500 and the number of features to 25 for each tree. Accuracy was determined as the root-mean-square error (RMSE), calculated using the RMSE function from the yardstick package in R.

Additionally, predicted antigenic distances of the out-of-bag samples were compared to the observed distances by fitting a linear model and calculating the R^2 value. To calculate the importance of each feature (X_i), the following metrics were calculated using the measure importance function of the randomForestExplainer package in R:

- – mean minimal depth: mean of the depths of the node in each tree that splits on this feature and is the closest to the root of the tree (minimal depth). The lower, the more important the feature since a low depth means that many observations are divided into groups based on this feature.
- – mse decrease: mean decrease of accuracy in predictions on out of bag samples when the feature is excluded from the model. The higher, the more important the feature.
- – number of nodes: total number of nodes in the forest that use the feature for splitting. The higher, the more important the feature.

The data and code used for the generation of the rf model is available at *https://github.com/SaelensLAB/RF*.

Acknowledgements

We gratefully acknowledge all data contributors, i.e., the Authors and their Originating laboratories responsible for obtaining the specimens, and their Submitting laboratories for generating the genetic sequence and metadata and sharing via the GISAID Initiative, on which this research is based. We are grateful to the animal caretakers of the animal house at the VIB-UGent Center for Inflammation Research.

Competing interests

XS reports grants from Sanofi Vaccines. GCG, TS, RG, JH, JC, IVU, TF, SS, SR, LR, and TUV are or were Sanofi employees and may hold shares and/or stock options in the company.

Disclosure of funding sources

This work was funded by Sanofi Vaccines.

Author Contributions

JPPC, TY, AS, IVU, TF, RG, JH, SS, SR, LL and JC performed experimental work. JPPC, TY, AS, RG, GCG, TUV, and XS designed the experiments, analyzed and interpreted the data. JM and MV analyzed the data. JPPC and XS wrote the manuscript and are accountable for accuracy and integrity of the work. All authors proofread and critically reviewed the manuscript.

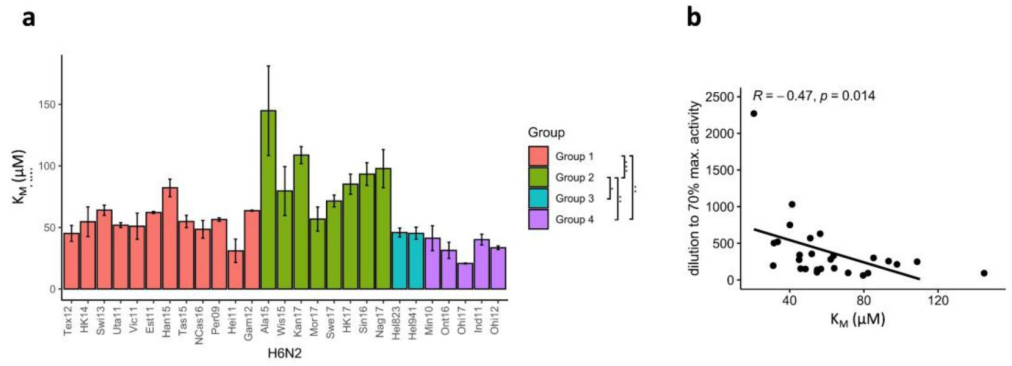

Figure 2 supplement 1.

The N2 NA substrate affinity is distinct in the N2 phylogenetic groups.

(a) K_M was determined for each H6N2 reassortant virus using the fluorogenic substrate MUNANA. N2 NAs are coloured according to the phylogenetic groups. Global test comparing the 4 groups was done using ANOVA (P= 2.4e-05) and pairwise comparison performed using Wilcoxon, ***P< 0.001, **P< 0.01, *P< 0.05. (b) Scatter-plot and correlation between the K_M values and dilutions required to obtain 70% max activity in ELLA.

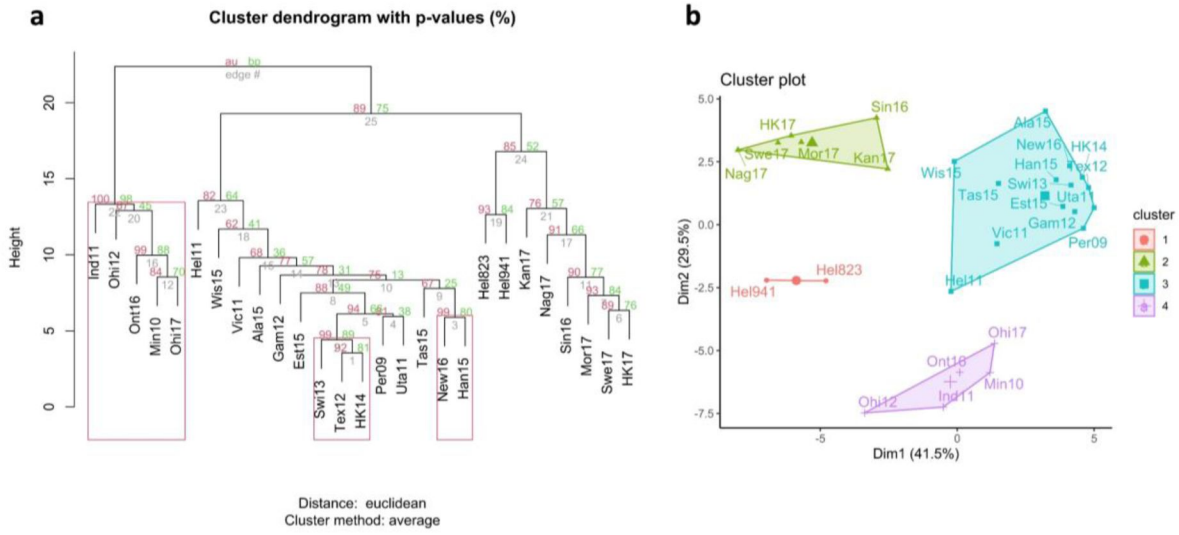

Figure 2 supplement 2.

Antigenic relationship between NA of the H6N2 viruses.

(a) Hierarchical clustering based on multisampling and multiscale bootstrap resampling. Approximately unbiased p-values (AU) are shown in red, bootstrap values in green, and edge values in grey. The red brackets represent the clusters with AU > 95%. (b) K-means clustering represented using principal component analysis (k=4).

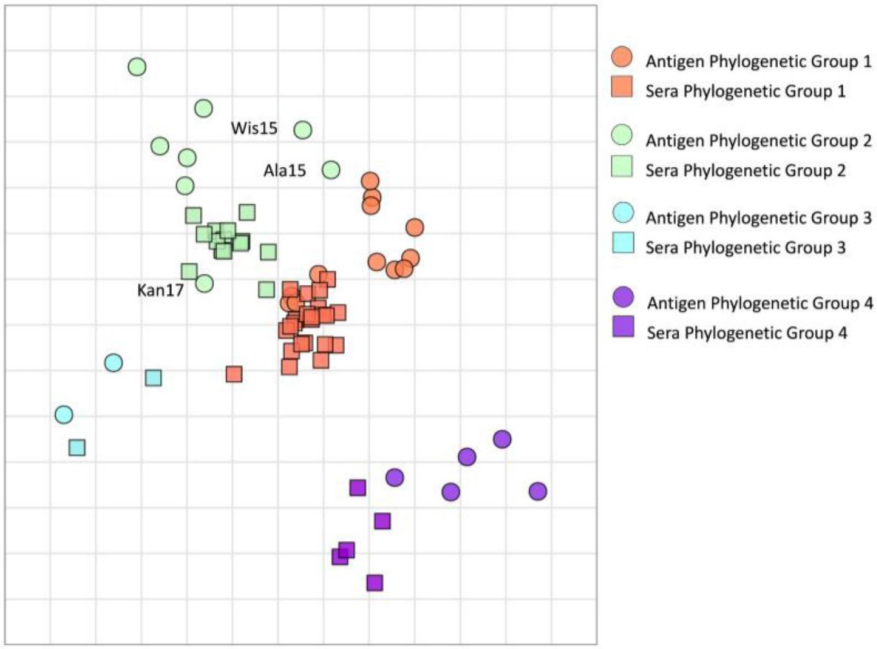

Figure 2 supplement 3.

Antigenic map of N2 NAs.

Antigen and sera distances are represented in the graph and coloured according to distinct phylogenetic groups. The spacing between grid lines is 1 unit of antigenic distance corresponding to a twofold dilution of immune serum in the NAI assay.

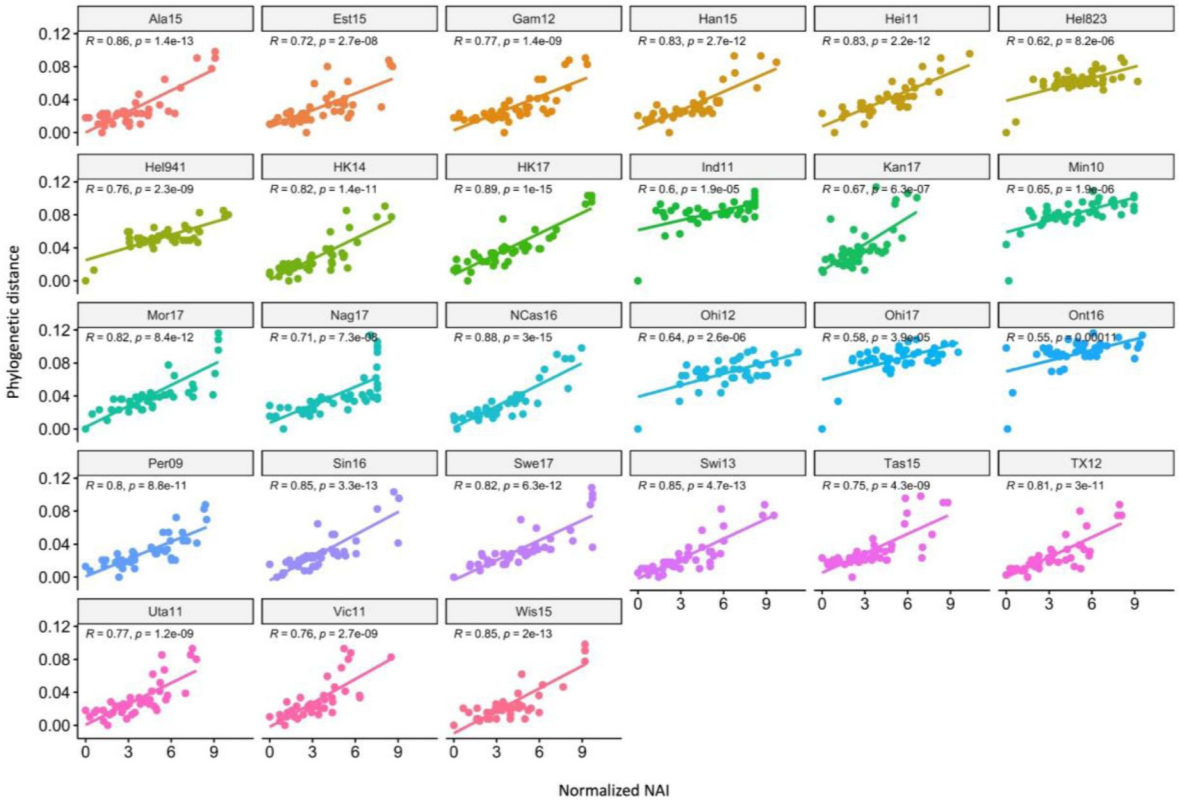

Figure 2 supplement 4.

Correlation of NAI fold reduction and phylogenetic relatedness.

The scatter plots show the phylogenetic distances (y-axis) and Normalized NAI as fold reduction relative to the maximal inhibition [$\log_2$ (max NAI/NAI)] (x-axis). Each graph represents one of the 27 H6N2s that were tested.

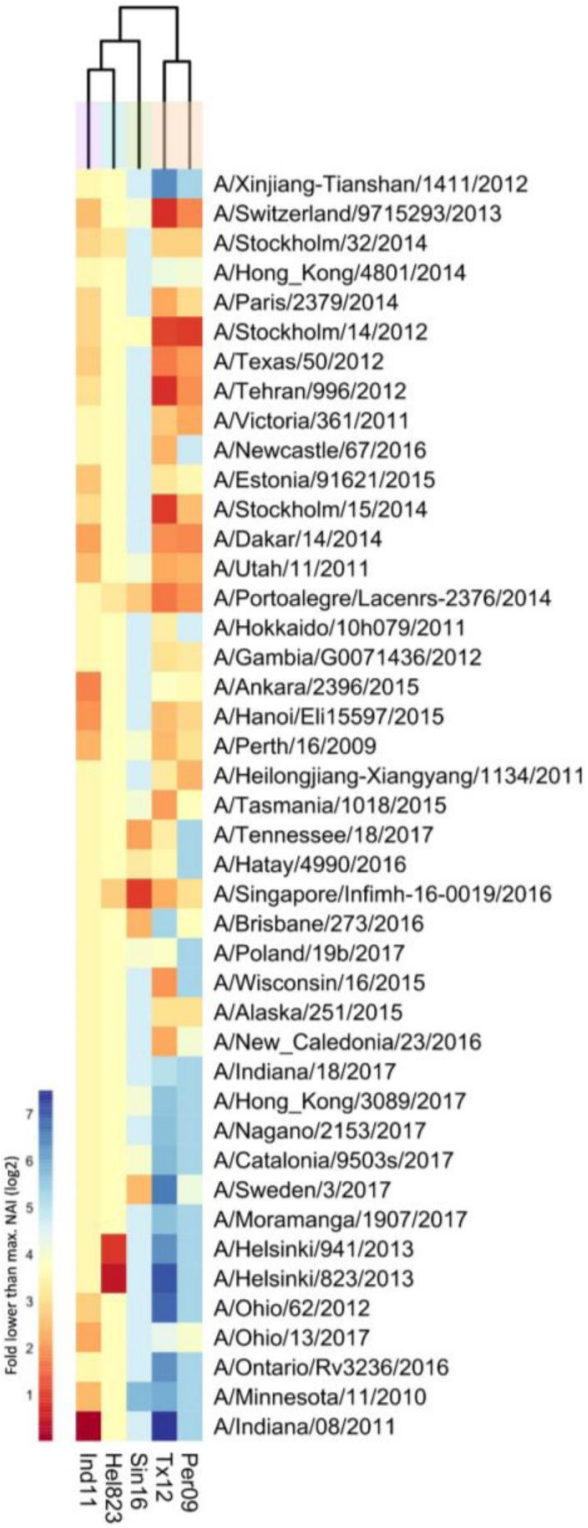

Figure 2 supplement 5.

Breadth of N2 inhibition of sera from ferrets primed by H1N2 infection only.

43 Heat-map representing the average of normalized neuraminidase inhibition per H6N2 [$\log_2$ (max NAI/NAI)] determined in ferret sera 2 weeks after infection. The red-to-blue scale indicates the fold reduction compared to the max NAI observed in ELLA against the H6N2 reassortants (listed at the bottom). UPGMA clustering of H6N2 inhibition profiles are shown on top of the heat map and coloured according to the phylogenetic groups.

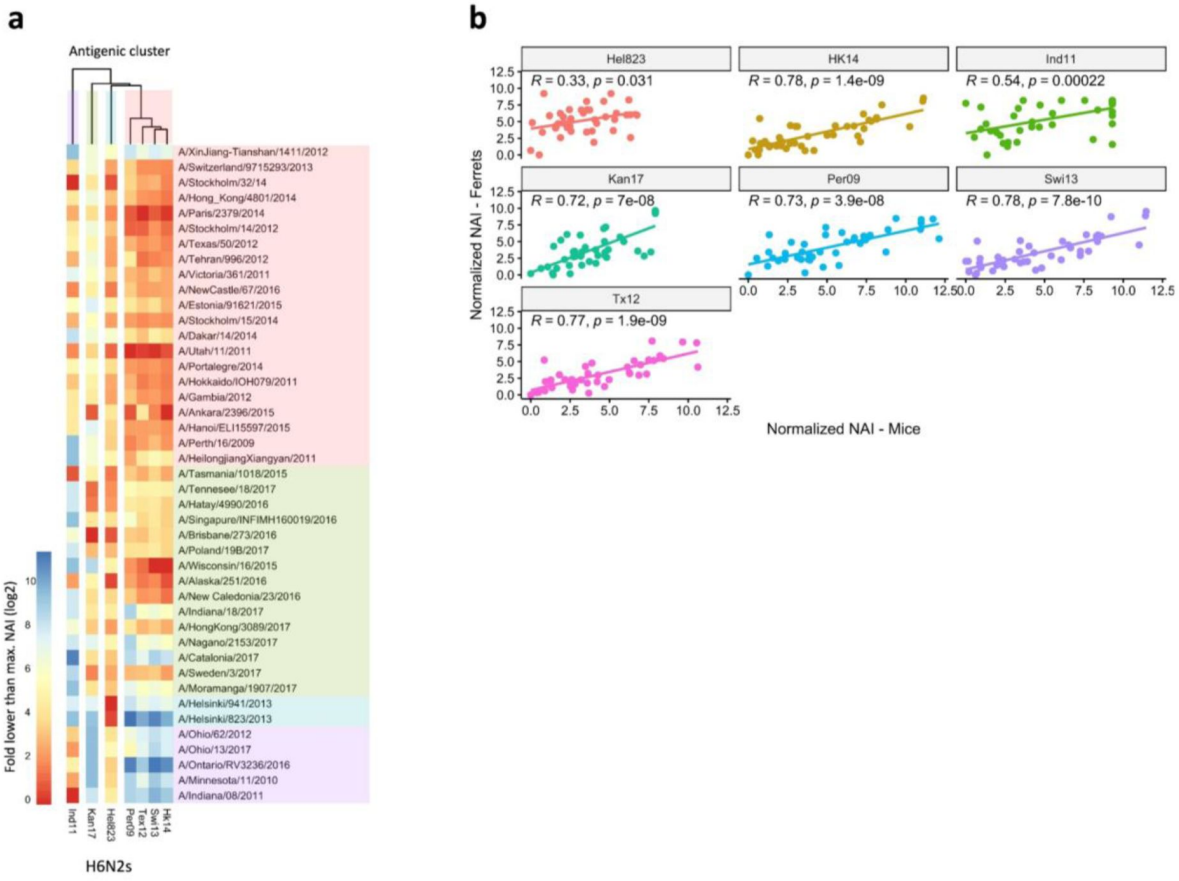

Figure 2 supplement 6.

Breadth of N2 inhibition is confirmed in mouse sera.

43 Heat-map representing the average of normalized neuraminidase inhibition per H6N2 [$\log_2$ (max NAI/NAI)] determined in mice sera after the boost (listed on the right). The red-to-blue scale indicates low-to-high NAI observed in ELLA against the H6N2 reassortants (listed at the bottom). UPGMA clustering of H6N2 inhibition profiles are shown on top of the heat map and coloured according to the phylogenetic groups. (b) **Correlation of NAI between mice and ferrets**. Scatter plot shows the normalized NAI as fold reduction from maximal inhibition [$\log_2$ (max NAI/NAI)] from ferrets (y-axis) versus mice (x-axis). The 7 H6N2s tested are indicated in the graphs.

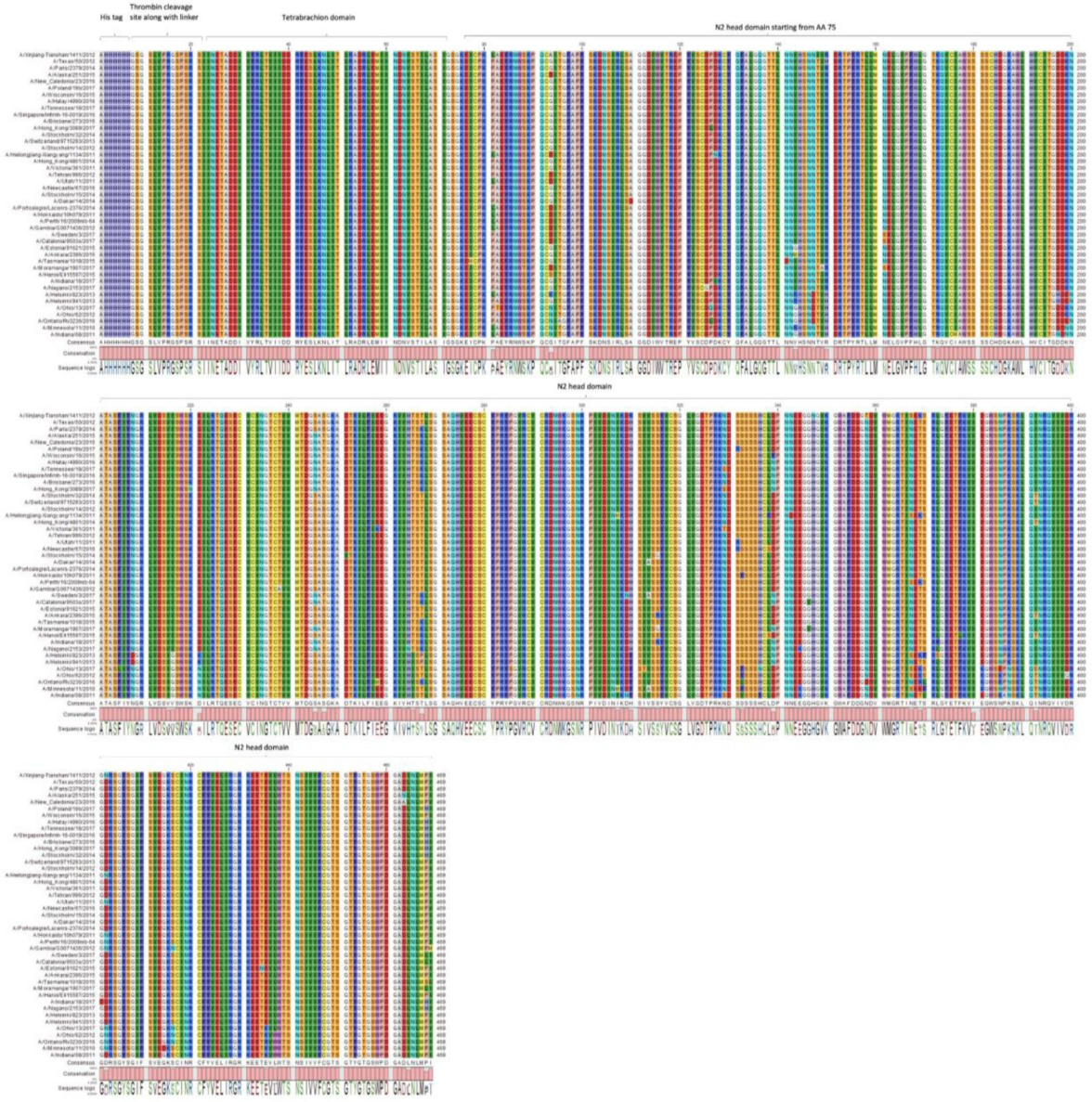

Figure 3 supplement 1.

Protein sequence alignment of N2 NACHO panel used for immunization.

The sequence of recombinant NA that was used for boosting ferrets or to prime/boost BALB/c mice was aligned starting from the HIS-tag, tetrabrachion and followed by NA head domain, as depicted on top of the sequences.

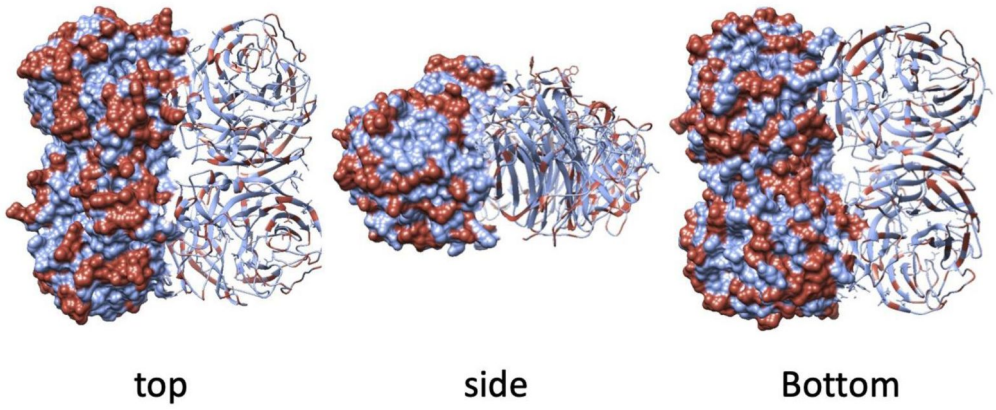

Figure 3 supplement 2.

Geometrical distribution of amino acid substitutions in the N2 structure.

The surface and ribbon representation indicate the geometrical distribution of the amino acid substitutions that are present in the panel of 43 N2 NAs used as immunogens in the study. Substitutions are highlighted in red on the model structure of N2 from H2N2 (A/RI/5+/1957, PBD 4H53).

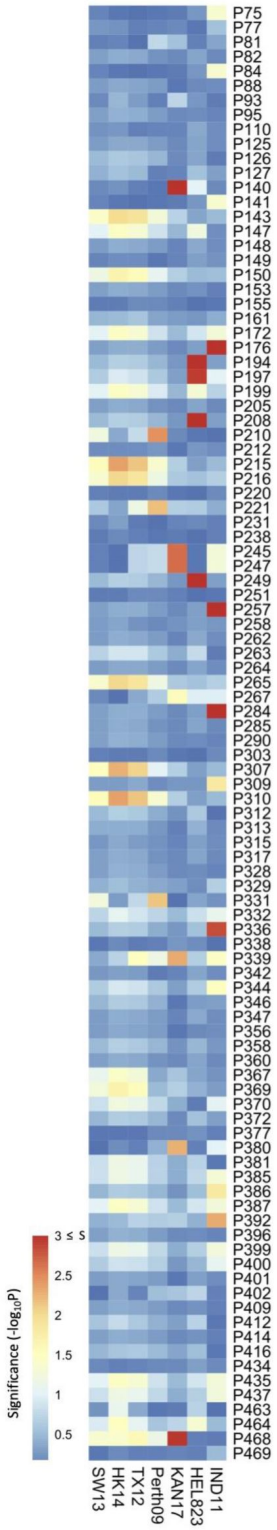

Figure 3 supplement 3.

Association study was performed on data obtained from mouse sera.

(a) Association study performed for each H6N2 virus (listed at the bottom) to determine the probability of each variable amino acid (listed on the right) present in the panel of 43 NAs to impact NAI. The red-to-blue scale represents significance values ($-\log_{10}P$) associated with each variable amino acid.

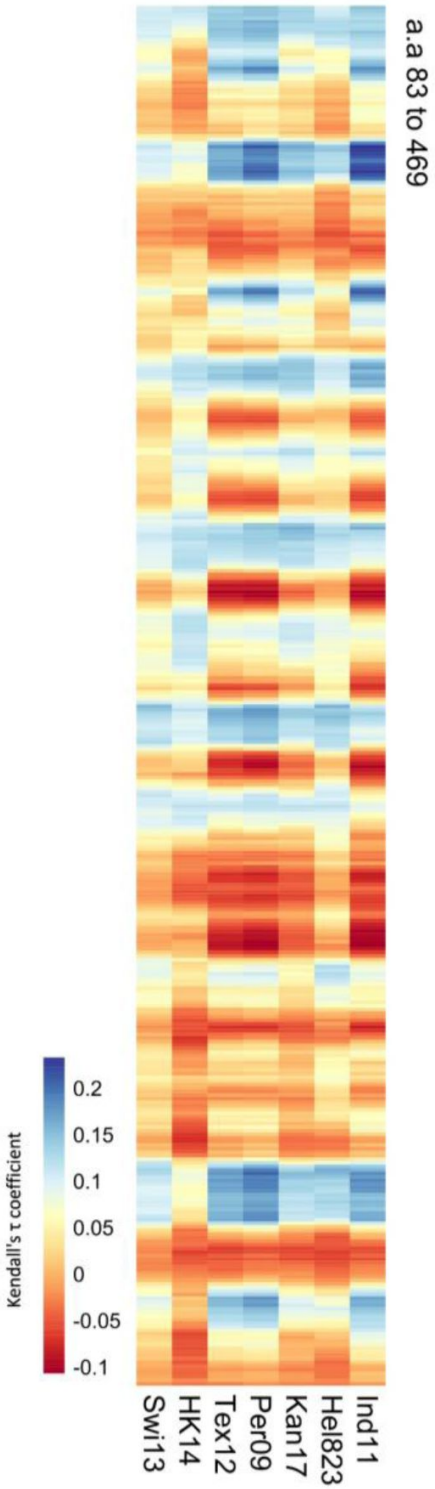

Figure 4 supplement 1.

Correlation of values obtained from the mouse sera panel and amino acid distances.

(a) Significance values (102 variable amino acids) obtained from the association study were correlated to the distance between every amino acid and each of the variable amino acids in the NA structure. The red-to-blue scale represents the Tau values obtained in the Kendall correlation. Amino acids 83 to 469 are shown from top to bottom of the heatmap. The H6N2s used in the NAI panel are listed at the bottom.

H3N2 strain NA source	Specific Activity nmole/min.µg
A/Stockholm/32/2014	9,62
A/Switzerland/9715293/2013	6,52
A/Hong Kong/4801/2014	4,13
A/Paris/2379/2014	2,42
A/Texas/50/2012	5,21
A/Stockholm/14/2012	2,42
A/Tehran/996/2012	8,46
A/Victoria/361/2011	2,71
A/Newcastle/67/2016	3,22
A/Estonia/91621/2015	5,3
A/Ankara/2396/2015	2,62
A/Stockholm/15/2014	1,14
A/Dakar/14/2014	2,37
A/PortoAlegre/Lacenrs-2376/2014	2,55
A/Utah/11/2011	1,40
A/Hokkaido/IOH079/2011	0,84
A/Gambia/G0071436/2012	1,60
A/Hanoi/Eli15597/2015	3,29
A/XinJiang-Tianshan/1411/2012	0,27
A/Perth/16/2009nib-64	5,3
A/Tasmania/1018/2015	27,48
A/NewCaledonia/23/2016	8,55
A/Alaska/251/2015	4,29
A/Hatay/4990/2016	5,83
A/Tennessee/18/2017	5,99
A/Singapore/Infimh160019/2016	8,01
A/Brisbane/273/2016	6,94
A/Poland/19b/2017	5,81
A/Wisconsin/16/2015	1,40
A/Indiana/08/2011	4,13
A/Hong-Kong/3089/2017	6,17
A/Nagano/2153/2017	2,29
A/Sweden/3/2017	2,76
A/Catalonia/9503s/2017	1,31
A/Moramanga/1907/2017	2,09
A/Heilongjiang_Xiangyan/1134/2011	6,61
A/Helsinki/823/2013	6,53
A/Helsinki/941/2013	7,02
A/Ohio/13/2017	2,59

Table S1.

Specific activity of the recombinant NACHOs.

A/Ohio/62/2012	4,28
A/Ontario/RV3236/2016	3,89
A/Indiana/18/2017	4,27
A/Minnesota/11/2010	4,25

Table S1. (continued)

H6Nx reassortant(*)	Titer (PFU/ml)	dilution to 70% max activity (ELLA)	K_M (MUNANA)
A/Ohio/62/2012 (Ohi12)	2.00E+08	2269.7	20.7
A/Indiana/08/2011 (Ind11)	2.50E+08	750.9	40.1
A/Ohio/13/2017 (Ohi17)	3.00E+08	521.5	33.5
A/Ontario/Rv3236/2016 (Ont16)	1.75E+08	504.1	31.5
A/Minnesota/11/2010 (Min10)	2.00E+08	1031.4	41.3
A/Helsinki/823/2013 (Hel823)	1.50E+08	155.2	45.9
A/Helsinki/941/2013 (Hel941)	3.50E+08	341.6	45.3
A/Nagano/2153/2017 (Nag17)	2.50E+08	213.6	97.8
A/Singapore/Infimh-16-0019/2016 (Sin16)	6.50E+07	257.1	93.3
A/Hong_Kong/3089/2017 (HK17)	2.00E+08	301.6	85.2
A/Sweden/3/2017 (Swe17)	6.00E+08	97	71.5
A/Moramanga/1907/2017 (Mor17)	1.40E+08	151.4	56.8
A/Kansas/14/2017 (Kan17)	2.50E+08	249	108.7
A/Wisconsin/16/2015 (Wis15)	2.00E+08	63.3	79.6
A/Gambia/G0071436/2012 (Gam12)	2.50E+08	331.5	63.6
A/Heilongjiang-Xiangyang/1134/2011 (Hei11)	2.10E+08	195.6	31.1
A/Perth/16/2009 (Per09)	3.20E+08	630.8	56.4
A/Newcastle/67/2016 (NCas16)	1.50E+08	150.4	48.5
A/Tasmania/1018/2015 (Tas15)	1.70E+08	139.5	54.8
A/Hanoi/Eli15597/2015 (Han15)	1.40E+08	94.6	82.2
A/Alaska/251/2015 (Ala15)	4.50E+08	93.7	144.8
A/Estonia/91621/2015 (Est15)	2.00E+08	281.9	62.1
A/Victoria/361/2011 (Vic11)	3.00E+08	570.3	51.1
A/Utah/11/2011 (Uta11)	2.50E+08	356.3	51.9
A/Switzerland/9715293/2013 (Swi13)	2.70E+08	160.8	64
A/Hong Kong/4801/2014 (HK14)	4.00E+07	106.3	54.7
A/Texas/50/2012 (Tex12)	2.00E+08	276.6	45.1

*Name of the virus from which the N2 NA in H6N2 reassortant virus was derived. The short name as used in the manuscript text is mentioned between brackets.

Table S2.

H6N2 reassortant viruses used in the ELLA assay.

Sera	Swi13	HK14	Tex12	Vic11	Ncas16	Est15	Uta11	Gam12	Han15	Hei11	Per09	Tas15	Ala15
A/Switzerland/9715293/2013	**9333.0**	6833.5	10301.6	2442.3	1489.8	5530.4	1460.6	3489.9	5253.8	1510.9	1899.6	1649.9	1812.3
A/Hong_Kong/4801/2014	7527.5	**10566.4**	14983.0	2559.1	4579.4	7944.5	3590.3	7065.0	4798.3	1971.2	2522.9	3842.2	4980.9
A/Texas/50/2012	10751.3	10397.6	**8843.5**	2089.6	740.9	3821.0	902.1	1519.1	1453.1	1112.9	2506.5	835.8	1490.8
A/Victoria/361/2011(Ivr-165)	16804.7	11568.3	11892.0	**3863.7**	1868.9	3480.4	2250.0	670.9	3963.3	1379.1	2888.7	883.1	1531.9
A/Newcastle/67/2016	7647.2	9702.6	5244.0	1056.9	**4218.8**	2295.9	5477.0	821.2	1515.9	1254.3	1304.0	1253.1	1021.6
A/Estonia/91621/2015	1277.1	1379.5	911.1	387.1	290.5	**2832.9**	277.9	335.3	225.6	272.5	193.3	217.2	70.9
A/Utah/11/2011	6121.8	6591.4	6253.2	3392.5	1570.0	3727.5	**2893.7**	1294.7	2496.3	4050.7	2196.7	376.0	869.2
A/Gambia/G0071436/2012	5513.7	6192.0	5040.0	1226.5	1492.3	6342.9	772.9	**730.2**	863.5	1810.2	1399.4	836.9	888.0
A/Hanoi/Eli15597/2015	4635.2	8150.5	6232.1	872.7	1617.0	7192.3	1023.4	1343.3	**1822.0**	1969.9	1168.3	1307.0	2383.4
A/Heilongjiang-Xiangyang/1134/2011	3506.3	3480.2	5123.0	3514.3	356.0	976.7	1657.1	245.9	557.9	**7094.8**	2056.7	168.3	658.3
A/Perth/16/2009nib-64	4961.8	13872.0	8102.7	2771.2	630.3	3502.5	2644.5	1079.5	441.6	1663.8	**2458.4**	418.4	748.3
A/Tasmania/1018/2015	6503.6	7894.2	5204.6	1298.1	2335.3	2927.7	1349.1	6451.6	2374.2	709.1	2659.2	**1150.5**	977.3
A/Alaska/251/2015	7291.7	8216.5	7274.8	1247.6	1050.4	7445.9	1975.1	348.6	1070.2	1828.5	1142.7	2300.4	**3418.1**
A/Singapore/Infimh-16-0019/2016	2564.5	3869.9	3206.3	1119.2	1038.5	732.7	545.2	252.3	1308.7	196.5	328.1	399.6	778.4
A/Wisconsin/16/2015	6157.8	6249.7	3088.6	693.4	998.2	1259.1	383.6	73.1	595.7	362.7	415.4	442.8	723.5
A/Hong_Kong/3089/2017	713.6	1372.5	1290.5	391.8	312.4	670.9	231.0	144.6	161.5	143.3	88.2	317.5	702.9
A/Nagano/2153/2017	784.6	798.8	567.6	102.6	215.5	530.1	158.5	97.5	182.8	145.2	108.7	172.4	332.8
A/Sweden/3/2017	2250.6	1249.6	2688.6	1818.4	785.2	443.3	632.2	726.1	3344.3	553.2	512.0	910.7	2153.6
A/Moramanga/1907/2017	1126.6	1371.0	720.8	205.3	185.9	1073.8	339.2	212.5	335.6	228.0	201.0	396.1	603.7
A/Helsinki/823/2013	1130.4	1408.4	1382.9	491.8	77.1	1930.9	324.0	141.1	133.6	431.4	289.4	90.0	106.9
A/Helsinki/941/2013	391.1	379.7	662.2	345.4	19.2	837.0	227.2	32.7	25.7	72.6	111.1	23.7	58.9
A/Ohio/13/2017	396.6	554.6	500.2	247.4	56.6	377.9	185.1	112.0	75.2	168.4	219.8	80.1	<20
A/Ohio/62/2012	445.7	644.5	694.0	157.0	33.1	1024.6	207.9	37.9	77.9	98.5	152.6	86.9	22.5
A/Ontario/Rv3236/2016	54.0	99.2	101.7	218.0	<20	51.7	43.8	<20	<20	<20	36.9	41.1	<20
A/Indiana/08/2011	34.4	72.5	110.4	177.3	22.4	43.1	46.8	31.4	<20	40.6	36.4	<20	<20
A/Minnesota/11/2010	59.4	146.7	91.6	<20	<20	44.0	39.0	<20	<20	41.1	30.8	<20	<20

Table S3.

NAI titers against H6N2 viruses of ferret sera obtained after the boost (Part I of II).

Sera	Sin16	Wis15	HK17	Nag17	Swe17	Mor17	Hel823	Hel941	Ohi17	Ohi12	Ont16	Ind11	Min11
A/Switzerland/9715293/2013	1291.6	939.6	1097.8	210.5	514.9	460.1	160.2	706.4	422.8	1072.5	354.5	227.5	302.5
A/Hong_Kong/4801/2014	636.5	780.7	1312.1	30.8	178.6	231.7	55.5	229.9	221.4	143.0	122.2	93.4	307.2
A/Texas/50/2012	436.8	556.3	462.7	<20	242.5	288.5	53.2	656.4	73.0	295.0	482.4	<20	149.6
A/Victoria/361/2011(Ivr-165)	568.2	1881.1	1227.3	108.5	293.8	407.7	79.3	1203.0	290.1	561.0	793.8	125.4	393.1
A/Newcastle/67/2016	192.6	246.4	411.3	18.3	70.8	125.6	206.8	259.5	893.7	1553.0	1089.8	<20	1619.5
A/Estonia/91621/2015	133.6	137.5	252.2	<20	78.5	<20	112.6	76.3	96.2	268.4	110.6	38.7	83.6
A/Utah/11/2011	212.4	753.0	215.9	41.4	138.5	265.5	100.4	549.1	208.9	1246.7	922.8	240.0	466.7
A/Gambia/G0071436/2012	390.8	532.3	694.8	37.3	174.6	139.2	296.9	470.4	233.7	154.4	423.5	157.8	709.3
A/Hanoi/Eli15597/2015	225.9	629.8	592.7	152.6	318.2	174.4	216.5	209.5	615.2	207.1	556.5	1205.8	669.2
A/Heilongjiang-Xiangyang/1134/2011	79.9	257.3	65.1	<20	77.1	34.9	475.2	76.0	236.7	1330.2	70.6	48.1	127.2
A/Perth/16/2009nib-64	263.1	535.5	249.8	<20	102.5	103.7	552.5	519.6	250.2	418.2	81.2	113.6	161.1
A/Tasmania/1018/2015	714.6	342.3	1149.8	178.8	321.5	551.2	363.1	1440.4	407.4	2702.2	819.1	463.8	689.9
A/Alaska/251/2015	655.6	1029.8	579.3	451.3	764.5	396.5	111.7	468.9	<20	72.8	88.1	<20	22.4
A/Singapore/Infimh-16-0019/2016	**3746.2**	1772.7	7210.9	1390.6	1637.5	1258.2	151.7	2123.3	94.6	282.6	68.0	<20	122.3
A/Wisconsin/16/2015	772.0	**5850.3**	678.1	373.4	680.7	420.1	<20	134.2	<20	74.7	<20	<20	<20
A/Hong_Kong/3089/2017	1534.5	708.7	**4119.2**	762.8	2114.3	744.7	297.3	324.9	<20	<20	<20	<20	<20
A/Nagano/2153/2017	501.4	157.0	1131.7	**960.8**	258.6	313.2	94.3	115.9	85.6	136.8	<20	<20	54.6
A/Sweden/3/2017	5336.2	1167.5	7099.8	1132.6	**8452.0**	4595.1	506.4	2310.2	133.0	199.5	323.9	27.2	58.5
A/Moramanga/1907/2017	1060.6	273.0	3033.6	258.9	1286.0	**6330.8**	75.6	143.2	57.3	106.0	96.7	<20	70.4
A/Helsinki/823/2013	519.3	215.9	745.1	<20	326.8	113.1	**5933.4**	11949.0	33.1	87.9	85.5	32.4	46.8
A/Helsinki/941/2013	257.3	79.5	156.3	<20	153.0	<20	3729.4	**17816.2**	<20	64.1	<20	<20	<20
A/Ohio/13/2017	28.9	<20	<20	<20	<20	<20	221.2	137.9	**2567.9**	28683.0	4819.3	781.1	4943.5
A/Ohio/62/2012	<20	<20	<20	<20	<20	<20	77.1	70.1	5592.0	**3811.0**	397.1	281.1	921.4
A/Ontario/Rv3236/2016	<20	<20	<20	<20	<20	<20	22.4	21.3	194.8	1500.5	**6167.6**	159.3	846.2
A/Indiana/08/2011	<20	<20	<20	<20	<20	<20	<20	<20	146.4	3741.8	486.8	**2910.9**	2498.3
A/Minnesota/11/2010	<20	<20	<20	<20	<20	<20	55.0	<20	202.3	509.1	726.6	380.2	**4375.6**

Table S3.

NAI titers against H6N2 viruses of ferret sera obtained after the boost (Part II of II).

References

Air GM, Els MC, Brown LE, Laver WG, Webster RG (1985) **Location of antigenic sites on the three-dimensional structure of the influenza N2 virus neuraminidase** *Virology* **145**:237–248 https://doi.org/10.1016/0042-6822(85)90157-6

Altman MO, Bennink JR, Yewdell JW, Herrin BR (2015) **Lamprey VLRB response to influenza virus supports universal rules of immunogenicity and antigenicity** *eLife* **4** https://doi.org/10.7554/eLife.07467

Bedford T, Suchard MA, Lemey P, Dudas G, Gregory V, Hay AJ, McCauley JW, Russell CA, Smith DJ, Rambaut A (2014) **Integrating influenza antigenic dynamics with molecular evolution** *eLife* **3** https://doi.org/10.7554/eLife.01914

Belongia EA, Simpson MD, King JP, Sundaram ME, Kelley NS, Osterholm MT, McLean HQ (2016) **Variable influenza vaccine effectiveness by subtype: a systematic review and meta-analysis of test-negative design studies** *The Lancet Infectious Diseases* **16**:942–951 https://doi.org/10.1016/S1473-3099(16)00129-8

Bien J, Tibshirani R (2011) **Hierarchical Clustering With Prototypes via Minimax Linkage** *J Am Stat Assoc* **106**:1075–1084

Cai Z, Zhang T, Wan X-F (2012) **Antigenic Distance Measurements for Seasonal Influenza Vaccine Selection** *Vaccine* **30**:448–453 https://doi.org/10.1016/j.vaccine.2011.10.051

Caillet C, Piras F, Bernard M-C, de Montfort A, Boudet F, Vogel FR, Hoffenbach A, Moste C, Kusters I. (2010) **AF03-adjuvanted and non-adjuvanted pandemic influenza A (H1N1) 2009 vaccines induce strong antibody responses in seasonal influenza vaccine-primed and unprimed mice** *Vaccine* **28**:3076–3079 https://doi.org/10.1016/j.vaccine.2010.02.050

Catani JPP, Job ER, Ysenbaert T, Smet A, Ray S, LaRue L, Stegalkina S, Barro M, Vogel TU, Saelens X (2022) **Pre-existing antibodies directed against a tetramerizing domain enhance the immune response against artificially stabilized soluble tetrameric influenza neuraminidase** *npj Vaccines* **7**:1–9 https://doi.org/10.1038/s41541-022-00435-7

CDC (2023) **Novel Influenza A Virus Infections**

Chen YQ *et al.* (2018) **Influenza Infection in Humans Induces Broadly Cross-Reactive and Protective Neuraminidase-Reactive Antibodies** *Cell* **173**:417–429 https://doi.org/10.1016/j.cell.2018.03.030

Chivukula S *et al.* (2021) **Development of multivalent mRNA vaccine candidates for seasonal or pandemic influenza** *NPJ Vaccines* **6** https://doi.org/10.1038/s41541-021-00420-6

Couch RB, Atmar RL, Franco LM, Quarles JM, Wells J, Arden N, Niño D, Belmont JW (2013) **Antibody Correlates and Predictors of Immunity to Naturally Occurring Influenza in Humans and the Importance of Antibody to the Neuraminidase** *The Journal of Infectious Diseases* **207**:974–981 https://doi.org/10.1093/infdis/jis935

Cox RJ (2013) **Correlates of protection to influenza virus, where do we go from here?** *Hum Vaccin Immunother* **9**:405–408 https://doi.org/10.4161/hv.22908

de Vries E, Du W, Guo H, de Haan CAM (2020) **Influenza A Virus Hemagglutinin–Neuraminidase– Receptor Balance: Preserving Virus Motility** *Trends in Microbiology* **28**:57–67 https://doi.org/10.1016/j.tim.2019.08.010

Deroo T, Min Jou W, Fiers W (1996) **Recombinant neuraminidase vaccine protects against lethal influenza** *Vaccine* **14**:561–569 https://doi.org/10.1016/0264-410X(95)00157-V

Eickhoff TC, Meiklejohn G (1969) **Protection against Hong Kong influneza by adjuvant vaccine containing A2-Ann Arbor-67** *Bull World Health Organ* **41**:562–563

Elbe S, Buckland-Merrett G (2017) **Data, disease and diplomacy: GISAID's innovative contribution to global health** *Global Challenges* **1**:33–46 https://doi.org/10.1002/gch2.1018

Ellis D *et al.* (2022) **Structure-based design of stabilized recombinant influenza neuraminidase tetramers** *Nat Commun* **13** https://doi.org/10.1038/s41467-022-29416-z

Ge J *et al.* (2022) **The Antibody Response Against Neuraminidase in Human Influenza A (H3N2) Virus Infections During 2018/2019 Flu Season: Focusing on the Epitopes of 329-N-Glycosylation and E344 in N2** *Front Microbiol* **13** https://doi.org/10.3389/fmicb.2022.845088

Hadházi Á *et al.* (2018) **A Sulfonozanamivir Analogue Has Potent Anti-influenza Virus Activity** *ChemMedChem* **13**:785–789 https://doi.org/10.1002/cmdc.201800092

Hoffmann E, Neumann G, Kawaoka Y, Hobom G, Webster RG (2000) **A DNA transfection system for generation of influenza A virus from eight plasmids** *Proc Natl Acad Sci U S A* **97**:6108–6113 https://doi.org/10.1073/pnas.100133697

Jester BJ, Uyeki TM, Jernigan DB (2020) **Fifty Years of Influenza A(H3N2) Following the Pandemic of 1968** *Am J Public Health* **110**:669–676 https://doi.org/10.2105/AJPH.2019.305557

Kosikova M, Li L, Radvak P, Ye Z, Wan X-F, Xie H. (2018) **Imprinting of Repeated Influenza A/H3 Exposures on Antibody Quantity and Antibody Quality: Implications for Seasonal Vaccine Strain Selection and Vaccine Performance** *Clin Infect Dis* **67**:1523–1532 https://doi.org/10.1093/cid/ciy327

Krammer F, Fouchier RAM, Eichelberger MC, Webby RJ, Shaw-Saliba K, Wan H, Wilson PC, Compans RW, Skountzou I, Monto AS (2018) **NAction! How Can Neuraminidase-Based Immunity Contribute to Better Influenza Virus Vaccines?** *mBio* **9**:e02332–17 https://doi.org/10.1128/mBio.02332-17

Leneva IA, Roberts N, Govorkova EA, Goloubeva OG, Webster RG (2000) **The neuraminidase inhibitor GS4104 (oseltamivir phosphate) is efficacious against A/Hong Kong/156/97 (H5N1) and A/Hong Kong/1074/99 (H9N2) influenza viruses** *Antiviral Res* **48**:101–115 https://doi.org/10.1016/s0166-3542(00)00123-6

Maier HE *et al.* (2019) **Pre-existing anti-neuraminidase antibodies are associated with shortened duration of influenza A (H1N1)pdm virus shedding and illness in naturally infected adults** *Clinical Infectious Diseases* https://doi.org/10.1093/cid/ciz639

Marathe BM, Lévêque V, Klumpp K, Webster RG, Govorkova EA (2013) **Determination of Neuraminidase Kinetic Constants Using Whole Influenza Virus Preparations and Correction for Spectroscopic Interference by a Fluorogenic Substrate** *PLOS ONE* **8** https://doi.org/10.1371/journal.pone.0071401

Marsh G, Tannock G (2005) **The role of reverse genetics in the development of vaccines against respiratory viruses** *Expert Opin Biol Ther* **5**:369–380 https://doi.org/10.1517/14712598.5.3.369

Matrosovich MN, Matrosovich TY, Gray T, Roberts NA, Klenk H-D (2004) **Neuraminidase Is Important for the Initiation of Influenza Virus Infection in Human Airway Epithelium** *Journal of Virology* **78**:12665–12667 https://doi.org/10.1128/jvi.78.22.12665-12667.2004

Memoli MJ *et al.* (2016) **Evaluation of Antihemagglutinin and Antineuraminidase Antibodies as Correlates of Protection in an Influenza A/H1N1 Virus Healthy Human Challenge Model** *mBio* **7**:e00417–16 https://doi.org/10.1128/mBio.00417-16

Meyer AG, Wilke CO (2015) **Geometric Constraints Dominate the Antigenic Evolution of Influenza H3N2 Hemagglutinin** *PLOS Pathogens* **11** https://doi.org/10.1371/journal.ppat.1004940

Monto Arnold S, Kendal Alan P. (1973) **EFFECT OF NEURAMINIDASE ANTIBODY ON HONG KONG INFLUENZA. The Lancet** *Originally published as Volume* **1**:301–623 https://doi.org/10.1016/S0140-6736(73)92196-X

Monto AS, Petrie JG, Cross RT, Johnson E, Liu M, Zhong W, Levine M, Katz JM, Ohmit SE (2015) **Antibody to influenza virus neuraminidase: An independent correlate of protection** *Journal of Infectious Diseases* **212**:1191–1199 https://doi.org/10.1093/infdis/jiv195

Nachbagauer R *et al.* (2017) **Defining the antibody cross-reactome directed against the influenza virus surface glycoproteins** *Nat Immunol* **18**:464–473 https://doi.org/10.1038/ni.3684

Ng S *et al.* (2019) **Novel correlates of protection against pandemic H1N1 influenza A virus infection** *Nature Medicine* **25**:962–967 https://doi.org/10.1038/s41591-019-0463-x

Palese P, Tobita K, Ueda M, Compans RW (1974) **Characterization of temperature sensitive influenza virus mutants defective in neuraminidase** *Virology* **61**:397–410 https://doi.org/10.1016/0042-6822(74)90276-1

Potter BI *et al.* (2019) **Evolution and rapid spread of a reassortant A(H3N2) virus that predominated the 2017–2018 influenza season** *Virus Evol* **5** https://doi.org/10.1093/ve/vez046

Powell H, Pekosz A (2020) **Neuraminidase antigenic drift of H3N2 clade 3c.2a viruses alters virus replication, enzymatic activity and inhibitory antibody binding** *PLOS Pathogens* **16** https://doi.org/10.1371/journal.ppat.1008411

Rajendran M, Nachbagauer R, Ermler ME, Bunduc P, Amanat F, Izikson R, Cox M, Palese P, Eichelberger M, Krammer F (2017) **Analysis of anti-influenza virus neuraminidase antibodies in children, adults, and the elderly by ELISA and enzyme inhibition: Evidence for original antigenic sin** *mBio* **8** https://doi.org/10.1128/mBio.02281-16

Rosu ME, Kok A, Bestebroer TM, de Meulder D, Verveer EP, Pronk MR, Dekker LJM, Luider TM, Richard M (2022) **Contribution of Neuraminidase to the Efficacy of Seasonal Split Influenza Vaccines in the Ferret Model** *J Virol* **96** https://doi.org/10.1128/jvi.01959-21

Smith DJ, Lapedes AS, de Jong JC, Bestebroer TM, Rimmelzwaan GF, Osterhaus ADME, Fouchier RAM (2004) **Mapping the antigenic and genetic evolution of influenza virus** *Science* **305**:371–376 https://doi.org/10.1126/science.1097211

Uyeki TM, Hui DS, Zambon M, Wentworth DE, Monto AS (2022) **Influenza** *The Lancet* **400**:693–706 https://doi.org/10.1016/S0140-6736(22)00982-5

Vavricka CJ *et al.* (2013) **Influenza neuraminidase operates via a nucleophilic mechanism and can be targeted by covalent inhibitors** *Nature Communications* **4** https://doi.org/10.1038/ncomms2487

Viboud C, Grais RF, Lafont BAP, Miller MA, Simonsen L (2005) **Multinational Impact of the 1968 Hong Kong Influenza Pandemic: Evidence for a Smoldering Pandemic** *The Journal of Infectious Diseases* **192**:233–248 https://doi.org/10.1086/431150

Wan H *et al.* (2019) **The neuraminidase of A(H3N2) influenza viruses circulating since 2016 is antigenically distinct from the A/Hong Kong/4801/2014 vaccine strain** *Nature Microbiology* **4**:2216–2225 https://doi.org/10.1038/s41564-019-0522-6

Wan H *et al.* (2018) **Comparison of the Efficacy of N9 Neuraminidase-Specific Monoclonal Antibodies against Influenza A(H7N9) Virus Infection** *Journal of Virology* **92**:e01588–17 https://doi.org/10.1128/JVI.01588-17

Wang Y, Lei R, Nourmohammad A, Wu NC (2021) **Antigenic evolution of human influenza H3N2 neuraminidase is constrained by charge balancing** *eLife* **10** https://doi.org/10.7554/eLife.72516

Weiss CD *et al.* (2019) **Neutralizing and Neuraminidase Antibodies Correlate With Protection Against Influenza During a Late Season A/H3N2 Outbreak Among Unvaccinated Military Recruits** *Clinical Infectious Diseases* :1–7 https://doi.org/10.1093/cid/ciz1198

Westgeest KB *et al.* (2012) **Genetic evolution of the neuraminidase of influenza A (H3N2) viruses from 1968 to 2009 and its correspondence to haemagglutinin evolution** *J Gen Virol* **93**:1996–2007 https://doi.org/10.1099/vir.0.043059-0

Wohlbold TJ *et al.* (2017) **Broadly protective murine monoclonal antibodies against influenza B virus target highly conserved neuraminidase epitopes** *Nature Microbiology* **2**:1415–1424 https://doi.org/10.1038/s41564-017-0011-8

Wu NC, Otwinowski J, Thompson AJ, Nycholat CM, Nourmohammad A, Wilson IA (2020) **Major antigenic site B of human influenza H3N2 viruses has an evolving local fitness landscape** *Nat Commun* **11** https://doi.org/10.1038/s41467-020-15102-5

Yao Y, Li X, Liao B, Huang L, He P, Wang F, Jiasheng Yang, Sun H, Zhao Y, Jialiang Yang (2017) **Predicting influenza antigenicity from Hemagglutintin sequence data based on a joint random forest method** *Sci Rep* **7** https://doi.org/10.1038/s41598-017-01699-z

Yasuhara A, Yamayoshi S, Kiso M, Sakai-Tagawa Y, Koga M, Adachi E, Kikuchi T, Wang IH, Yamada S, Kawaoka Y (2019) **Antigenic drift originating from changes to the lateral surface of the neuraminidase head of influenza A virus** *Nature Microbiology* **4**:1024–1034 https://doi.org/10.1038/s41564-019-0401-1

Yen H-L, Herlocher LM, Hoffmann E, Matrosovich MN, Monto AS, Webster RG, Govorkova EA (2005) **Neuraminidase Inhibitor-Resistant Influenza Viruses May Differ Substantially in Fitness and Transmissibility** *Antimicrob Agents Chemother* **49**:4075–4084 https://doi.org/10.1128/AAC.49.10.4075-4084.2005

Article and author information

João Paulo Portela Catani
VIB Center for Medical Biotechnology, VIB, B-9052 Ghent, Belgium, Department of Biochemistry and Microbiology, Ghent University, B-9052 Ghent, Belgium

Anouk Smet
VIB Center for Medical Biotechnology, VIB, B-9052 Ghent, Belgium, Department of Biochemistry and Microbiology, Ghent University, B-9052 Ghent, Belgium

Tine Ysenbaert
VIB Center for Medical Biotechnology, VIB, B-9052 Ghent, Belgium, Department of Biochemistry and Microbiology, Ghent University, B-9052 Ghent, Belgium

Marnik Vuylsteke
Gnomixx, Melle, Belgium

Guy Bottu
VIB Bioinformatics Core, VIB, B-9052 Ghent, Belgium

Janick Mathys
VIB Bioinformatics Core, VIB, B-9052 Ghent, Belgium

Alexander Botzki
VIB Bioinformatics Core, VIB, B-9052 Ghent, Belgium

Guadalupe Cortes-Garcia
Sanofi, Research North America, Cambridge, Massachusetts, USA

Tod Strugnell
Sanofi, Research North America, Cambridge, Massachusetts, USA

Raul Gomila
Sanofi, Research North America, Cambridge, Massachusetts, USA

John Hamberger
Sanofi, Research North America, Cambridge, Massachusetts, USA

John Catalan
Sanofi, Research North America, Cambridge, Massachusetts, USA

Irina V. Ustyugova
Sanofi, Research North America, Cambridge, Massachusetts, USA

Timothy Farrell
Sanofi, Research North America, Cambridge, Massachusetts, USA

Svetlana Stegalkina
Sanofi, Research North America, Cambridge, Massachusetts, USA

Satyajit Ray
Sanofi, Research North America, Cambridge, Massachusetts, USA

Lauren LaRue
Sanofi, Research North America, Cambridge, Massachusetts, USA

Xavier Saelens
VIB Center for Medical Biotechnology, VIB, B-9052 Ghent, Belgium, Department of Biochemistry and Microbiology, Ghent University, B-9052 Ghent, Belgium
For correspondence: xavier.saelens@vib-ugent.be
ORCID iD: 0000-0002-3861-6965

Thorsten U. Vogel
Sanofi, Research North America, Cambridge, Massachusetts, USA
For correspondence: thorsten.vogel@sanofi.com

Copyright

© 2023, Catani et al.

This article is distributed under the terms of the Creative Commons Attribution License, which permits unrestricted use and redistribution provided that the original author and source are credited.

Editors

Reviewing Editor
Richard Neher
University of Basel, Basel, Switzerland

Senior Editor
Betty Diamond
The Feinstein Institute for Medical Research, Manhasset, United States of America

Reviewer #1 (Public Review):

Summary

The authors investigated the antigenic diversity of recent (2009-2017) A/H3N2 influenza neuraminidases (NAs), the second major antigenic protein after haemagglutinin. They used 27 viruses and 43 ferret sera and performed NA inhibition. This work was supported by a subset of mouse sera. Clustering analysis determined 4 antigenic clusters, mostly in concordance with the genetic groupings. Association analysis was used to estimate important amino acid positions, which were shown to be more likely close to the catalytic site. Antigenic distances were calculated and a random forest model used to determine potential important sites.

This revision has addressed many of my concerns of inconsistencies in the methods, results and presentation. There are still some remaining weaknesses in the computational work.

Strengths

(1) The data cover recent NA evolution and a substantial number (43) of ferret (and mouse) sera were generated and titrated against 27 viruses. This is laborious experimental work and is the largest publicly available neuraminidase inhibition dataset that I am aware of. As such, it will prove a useful resource for the influenza community.

(2) A variety of computational methods were used to analyse the data, which give a rounded picture of the antigenic and genetic relationships and link between sequence, structure and phenotype.

(3) Issues raised in the previous review have been thoroughly addressed.

Weaknesses:

Some concerns regarding the robustness of the machine learning model and potential overfitting remain.

https://doi.org/10.7554/eLife.90782.3.sa2

Reviewer #2 (Public Review):

Summary:

The authors characterized the antigenicity of N2 protein of 43 selected A(H3N2) influenza A viruses isolated from 2009-2017 using ferret and mice immune sera. Four antigenic groups were identified, which the authors claimed to be correlated with their respective phylogenic/genetic groups. Among 102 amino acids differed by the 44 selected N2 proteins, the authors identified residues that differentiate the antigenicity of the four groups and constructed a machine-learning model that provides antigenic distance estimation. Three recent A(H3N2) vaccine strains were tested in the model but there was no experimental data to confirm the model prediction results.

Strengths:

This study used N2 protein of 44 selected A(H3N2) influenza A viruses isolated from 2009-2017 and generated corresponding panels of ferret and mouse sera to react with the selected strains. The amount of experimental data for N2 antigenicity characterization is large enough for model building.

Weaknesses:

One weakness is the use of double-immune ferret sera (post-infection plus immunization with recombinant NA protein) or mouse sera (immunized twice with recombinant NA protein) to characterize the antigenicity of the selected A(H3N2) viruses. Conventionally, NA antigenicity is characterized using ferret sera after a single infection. Repeated influenza exposure in ferrets has been shown to enhance antibody binding affinity and may affect the cross-reactivity to heterologous strains (PMID: 29672713). The increased cross-reactivity is supported by the NAI titers shown in Table S3, as many of the double immune ferret sera showed the highest reactivity not against its own homologous virus but to heterologous strains. In response to the reviewer's comment, the authors agreed the use of double-immune ferret sera may be a limitation of the study.

Another weakness is that the authors used the newly constructed a model to predict antigenic distance of three recent A(H3N2) viruses but there is no experimental data to validate their prediction (eg. if these viruses are indeed antigenically deviating from group 2 strains as concluded by the authors). Leaving out data from some strains for testing is a useful check, but due to phylogenetic correlations in the data the generalizability of the machine learning is not guaranteed.

https://doi.org/10.7554/eLife.90782.3.sa1

Reviewer #3 (Public Review):

Summary:

This paper by Portela Catani et al examines the antigenic relationships (measured using monotypic ferret and mouse sera) across a panel of N2 genes from the past 14 years, along with the underlying sequence differences and phylogenetic relationships. This is a highly significant topic given the recent increased appreciation of the importance of NA as a vaccine target, and the relative lack of information about NA antigenic evolution compared with what is known about HA. Thus, these data will be of interest to those studying the antigenic evolution of influenza viruses. The methods used are generally quite sound, though there are a few addressable concerns that limit the confidence with which conclusions can be drawn from the data/analyses.

Strengths:

-The significance of the work, and the (general) soundness of the methods.
-Explicit comparison of results obtained with mouse and ferret sera

Weaknesses:

- Machine learning analyses neither experimentally validated nor shown to be better than simple, phylogenetic-based inference.

https://doi.org/10.7554/eLife.90782.3.sa0

Author response:

The following is the authors' response to the previous reviews.

> ***eLife assessment***
>
> *This study presents valuable data on the antigenic properties of neuraminidase proteins of human A/H3N2 influenza viruses sampled between 2009 and 2017. The antigenic properties are found to be generally concordant with genetic groups. Additional analysis have strengthened the revised manuscript, and the evidence supporting the claims is solid.*
>
> ***Public Reviews:***
>
> ***Reviewer #1 (Public Review):***
>
> *Summary*
>
> *The authors investigated the antigenic diversity of recent (2009-2017) A/H3N2 influenza neuraminidases (NAs), the second major antigenic protein after haemagglutinin. They*

> *used 27 viruses and 43 ferret sera and performed NA inhibition. This work was supported by a subset of mouse sera. Clustering analysis determined 4 antigenic clusters, mostly in concordance with the genetic groupings. Association analysis was used to estimate important amino acid positions, which were shown to be more likely close to the catalytic site. Antigenic distances were calculated and a random forest model used to determine potential important sites.*
>
> *This revision has addressed many of my concerns of inconsistencies in the methods, results and presentation. There are still some remaining weaknesses in the computational work.*
>
> *Strengths*
>
> *(1) The data cover recent NA evolution and a substantial number (43) of ferret (and mouse) sera were generated and titrated against 27 viruses. This is laborious experimental work and is the largest publicly available neuraminidase inhibition dataset that I am aware of. As such, it will prove a useful resource for the influenza community.*
>
> *(2) A variety of computational methods were used to analyse the data, which give a rounded picture of the antigenic and genetic relationships and link between sequence, structure and phenotype.*
>
> *(3) Issues raised in the previous review have been thoroughly addressed.*
>
> *Weaknesses*
>
> *(1). Some inconsistencies and missing data in experimental methods Two ferret sera were boosted with H1N2, while recombinant NA protein for the others. This, and the underlying reason, are clearly explained in the manuscript. The authors note that boosting with live virus did not increase titres. Additionally, one homologous serum (A/Kansas/14/2017) was not generated, although this would not necessarily have impacted the results.*

We agree with the reviewer and this point was addressed in the previous rebuttal.

> *(2) Inconsistency in experimental results*
>
> *Clustering of the NA inhibition results identifies three viruses which do not cluster with their phylogenetic group. Again this is clearly pointed out in the paper and is consistent with the two replicate ferret sera. Additionally, A/Kansas/14/2017 is in a different cluster based on the antigenic cartography vs the clustering of the titres*

We agree with the reviewer and this point was addressed in the previous rebuttal.

> *(3) Antigenic cartography plot would benefit from documentation of the parameters and supporting analyses*

a. The number of optimisations used

We used 500 optimizations. This information is now included in the Methods section.

b. The final stress and the difference between the stress of the lowest few (e.g. 5) optimisations, or alternatively a graph of the stress of all the optimisations. Information on the stress per titre and per point, and whether any of these were outliers

The stress was obtained from 1, 5, 500, or even 5000 optimizations (resulting in stress values of respectively, 1366.47, 1366.47, 2908.60, and 3031.41). Besides limited variation or non-

conversion of the stress values after optimization, the obtained maps were consistent in multiple runs. The map was obtained keeping the best optimization (stress value 1366.47, selected using the keepBestOptimization() function).

Author response image 1.

The stress per point is presented in the heat map below.

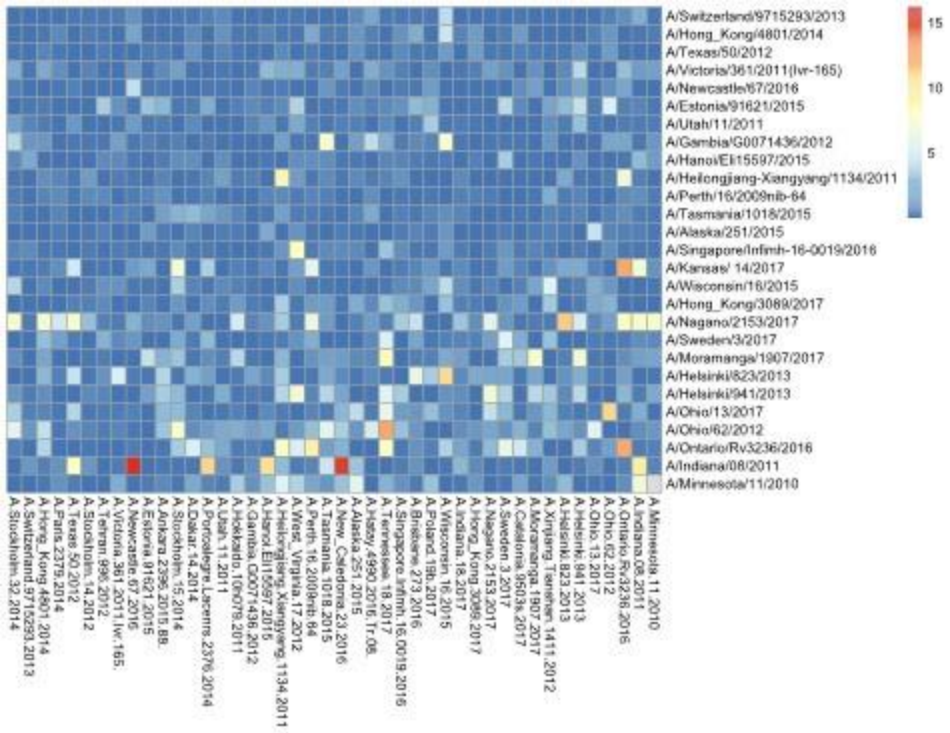

The heat map indicates stress per serum (x-axis) and strain (y-axis) in blue to red scale.

c. A measure of uncertainty in position (e.g. from bootstrapping)

Bootstrap was performed using 1000 repeats and 100 optimizations per repeat. The uncertainty is represented in the blob plot below.

Author response image 2.

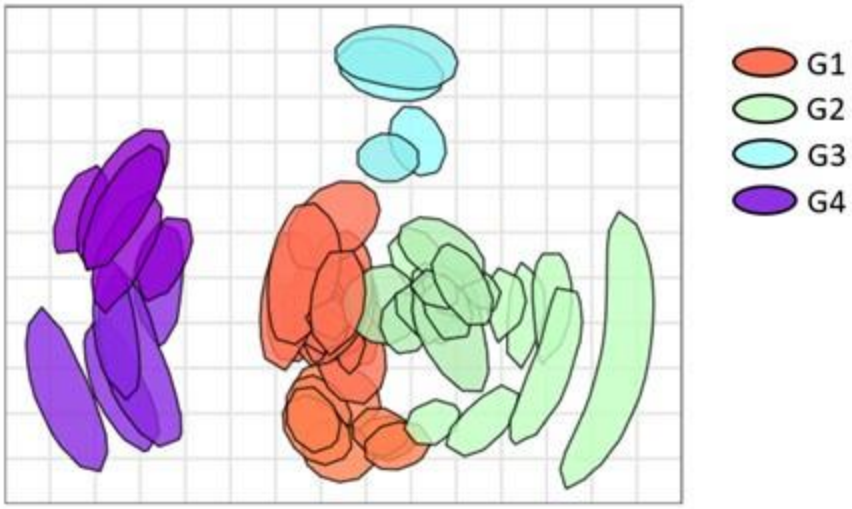

> *(4) Random forest*
>
> *The full dataset was used for the random forest model, including tuning the hyperparameters. It is more robust to have a training and test set to be able to evaluate overfitting (there are 25 features to classify 43 sera).*

Explicit cross validation is not necessary for random forests as the out of bag process with multiple trees implicitly covers cross validation. In the random forest function in R this is done by setting the mtry argument (number of variables randomly sampled as candidates at each split). R samples variables with replacement (the same variable can be sampled multiple times) of the candidates from the training set. RF will then automatically take the data that is not selected as candidates as test set. Overfit may happen when all data is used for training but the RF method implicitly does use a test set and does not use all data for training.

Code:

rf <- randomForest(X,y=Y,ntree=1500,mtry=25,keep.forest=TRUE,importance=TRUE)

> ***Reviewer #2 (Public Review):***
>
> ***Summary:***
>
> *The authors characterized the antigenicity of N2 protein of 43 selected A(H3N2) influenza A viruses isolated from 2009-2017 using ferret and mice immune sera. Four antigenic groups were identified, which the authors claimed to be correlated with their respective phylogenic/ genetic groups. Among 102 amino acids differed by the 44 selected N2 proteins, the authors identified residues that differentiate the antigenicity of the four groups and constructed a machine-learning model that provides antigenic distance estimation. Three recent A(H3N2) vaccine strains were tested in the model but there was no experimental data to confirm the model prediction results.*
>
> *Strengths:*
>
> *This study used N2 protein of 44 selected A(H3N2) influenza A viruses isolated from 2009-2017 and generated corresponding panels of ferret and mouse sera to react with the*

> *selected strains. The amount of experimental data for N2 antigenicity characterization is large enough for model building.*
>
> *Weaknesses:*
>
> *The main weakness is that the strategy of selecting 43 A(H3N2) viruses from 2009-2017 was not explained. It is not clear if they represent the overall genetic diversity of human A(H3N2) viruses circulating during this time. In response to the reviewer's comment, the authors have provided a N2 phylogenetic tree using180 randomly selected N2 sequences from human A(H3N2) viruses from 2009-2017. While the 43 strains seems to scatter across the N2 tree, the four antigenic groups described by the author did not correlated with their respective phylogenic/ genetic groups as shown in Fig. 2. The authors should show the N2 phylogenic tree together with Fig. 2 and discuss the discrepancy observed.*

The discrepancies between the provided N2 phylogenetic tree using 180 selected N2 sequences was primarily due to visualization. In the tree presented in Figure 2 the phylogeny was ordered according to branch length in a decreasing way. Further, the tree represented in the rebuttal was built with PhyML 3.0 using JTT substitution model, while the tree in figure 2 was build in CLC Workbench 21.0.5 using Bishop-Friday substitution model. The tree below was built using the same methodology as Figure 2, including branch size ordering. No discrepancies are observed.

> *Phylogenetic tree representing relatedness of N2 head domain. N2 NA sequences were ordered according to the branch length and phylogenetic clusters are colored as follows: G1: orange, G2: green, G3: blue, and G4: purple. NA sequences that were retained in the breadth panel are named according to the corresponding H3N2 influenza viruses. The other NA sequences are coded.*

Author response image 3.

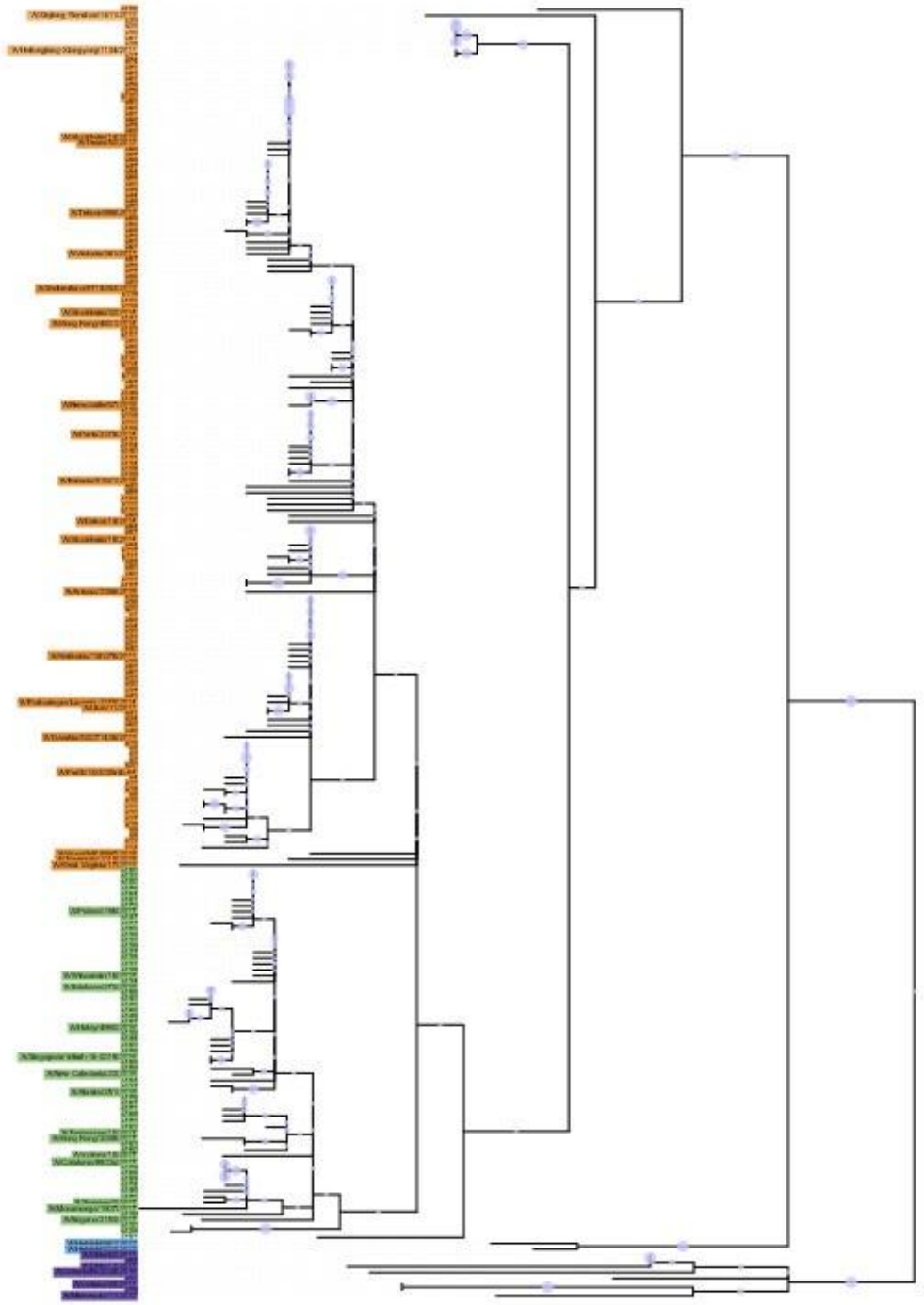

The second weakness is the use of double-immune ferret sera (post-infection plus immunization with recombinant NA protein) or mouse sera (immunized twice with recombinant NA protein) to characterize the antigenicity of the selected A(H3N2) viruses. Conventionally, NA antigenicity is characterized using ferret sera after a single infection. Repeated influenza exposure in ferrets has been shown to enhance antibody binding

> *affinity and may affect the cross-reactivity to heterologous strains (PMID: 29672713). The increased cross-reactivity is supported by the NAI titers shown in Table S3, as many of the double immune ferret sera showed the highest reactivity not against its own homologous virus but to heterologous strains. In response to the reviewer's comment, the authors agreed the use of double-immune ferret sera may be a limitation of the study. It would be helpful if the authors can discuss the potential effect on the use of double-immune ferret sera in antigenicity characterization in the manuscript.*

Our study was designed to understand the breadth of the anti-NA response after the incorporation of NA as a vaccine antigens. Our data does not allow to conclude whether increased breadth of protection is merely due to increased antibody titers or whether an NA boost immunization was able to induce antibody responses against epitopes that were not previously recognized by primary response to infection. However, we now mention this possibility in the discussion and cite Kosikova et al. CID 2018, in this context.

> *Another weakness is that the authors used the newly constructed a model to predict antigenic distance of three recent A(H3N2) viruses but there is no experimental data to validate their prediction (eg. if these viruses are indeed antigenically deviating from group 2 strains as concluded by the authors). In response to the comment, the authors have taken two strains out of the dataset and use them for validation. The results is shown as Fig. R7. However, it may be useful to include this in the main manuscript to support the validity of the model.*

The removal of 2 strains was performed to illustrate the predictive performance of the RF modeling. However, Random Forest does not require cross-validation. The reason is that RF modeling already uses an out-of-bag evaluation which, in short, consists of using only a fraction of the data for the creation of the decision trees (2/3 of the data), obviating the need for a set aside the test set:

"…In each bootstrap training set, about one-third of the instances are left out. Therefore, the out-of-bag estimates are based on combining only about one- third as many classifiers as in the ongoing main combination. Since the error rate decreases as the number of combinations increases, the out-of-bag estimates will tend to overestimate the current error rate. To get unbiased out-of-bag estimates, it is necessary to run past the point where the test set error converges. But unlike cross-validation, where bias is present but its extent unknown, the out-of-bag estimates are unbiased…" from https://www.stat.berkeley.edu/%7Ebreiman/randomforest2001.pdf

> ***Reviewer #3 (Public Review):***
>
> *Summary:*
>
> *This paper by Portela Catani et al examines the antigenic relationships (measured using monotypic ferret and mouse sera) across a panel of N2 genes from the past 14 years, along with the underlying sequence differences and phylogenetic relationships. This is a highly significant topic given the recent increased appreciation of the importance of NA as a vaccine target, and the relative lack of information about NA antigenic evolution compared with what is known about HA. Thus, these data will be of interest to those studying the antigenic evolution of influenza viruses. The methods used are generally quite sound, though there are a few addressable concerns that limit the confidence with which conclusions can be drawn from the data/analyses.*
>
> *Strengths:*

- *The significance of the work, and the (general) soundness of the methods. - Explicit comparison of results obtained with mouse and ferret sera*

Weaknesses:

- *Approach for assessing influence of individual polymorphisms on antigenicity does not account for potential effects of epistasis (this point is acknowledged by the authors).*

We agree with the reviewer and this point was addressed in the previous rebuttal.

- *Machine learning analyses neither experimentally validated nor shown to be better than simple, phylogenetic-based inference.*

We respectfully disagree with the reviewer. This point was addressed in the previous rebuttal as follows.

This is a valid remark and indeed we have found a clear correlation between NAI cross reactivity and phylogenetic relatedness. However, besides achieving good prediction of the experimental data (as shown in Figure 5 and in FigureR7), machine Learning analysis has the potential to rank or indicate major antigenic divergences based on available sequences before it has consolidated as new clade. ML can also support the selection and design of broader reactive antigens. “

Recommendations for the authors:

Reviewer #2 (Recommendations For The Authors):

(1) Discuss the discrepancy between Fig. 2 and the newly constructed N2 phylogenetic tree with 180 randomly selected N2 sequences of A(H3N2) viruses from 2009-2017. Specifically please explain the antigenic vs. phylogenetic relationship observed in Fig. 2 was not observed in the large N2 phylogenetic tree.

Discrepancies were due to different method and visualization. A new tree was provided.

(2) Include a sentence to discuss the potential effect on the use of double-immune ferret sera in antigenic characterization.

We prefer not to speculate on this.

(3) Include the results of the exercise run (with the use of Swe17 and HK17) in the manuscript as a way to validate the model.

The exercise was performed to illustrate predictive potential of the RF modeling to the reviewer. However, cross-validation is not a usual requirement for random forest, since it uses out-of-bag calculations. We prefer to not include the exercise runs within the main manuscript.